MOLECULAR AND CELLULAR LEVEL ADAPTATIONS OF BONE MARROW MESENCHYMAL PROGENITOR CELLS TO CHEMICAL AND PHYSICAL SIGNALS

A Thesis Submitted to
the Graduate School of Engineering and Science of
İzmir Institute of Technology
in Partial Fulfillment of the Requirement for the Degree of

DOCTOR OF PHILOSOPHY

in Bioengineering

by
Öznur BASKAN ERBİLGİÇ

December 2020
İZMİR

ACKNOWLEDGEMENT

I would like to offer my deepest and sincere gratitude to my supervisor Assoc. Prof. Dr. Engin ÖZÇİVİCİ for his supports, trust, critical discussions, understanding and patience throughout this study. I also would like to thank to him for his advice and belief in me throughout my life.

I would like to thank to my dissertation committee members Assoc. Prof. Dr. Özden YALÇIN ÖZUYSAL, Prof. Dr. Ataç SÖNMEZ, Asst. Prof. Dr. Nur Başak SÜRMELİ ERALTUĞ, Asst. Prof. Dr. Kemal Uğur TÜFEKÇİ and my co-advisor Prof. Dr. Neşe ATABEY.

I would also like to thank to Assoc. Prof. Dr Gülistan MEŞE ÖZÇİVİCİ and Assoc. Prof. Dr. Özden YALÇIN ÖZUYSAL for their critical comments and guidance in this study for their valuable advices during lab meetings and my research group members Özge KARADAŞ, previous member Melis OLÇUM UZAN, Müge ANIL İNEVİ, Öykü SARIGİL, special thanks to Yağmur Ceren ÜNAL for her help in formatting and giving the last shape of the thesis.

I would like to thank warmly to my husband Uğur ERBİLGİÇ, who suffers all of my whims and supports my decisions.

The biggest thanks are for my family. My parents Fehime and İlhami BASKAN were always by my side throughout my life and I felt their support every single day.

ABSTRACT

MOLECULAR AND CELLULAR LEVEL ADAPTATIONS OF BONE MARROW MESENCHYMAL PROGENITOR CELLS TO CHEMICAL AND PHYSICAL SIGNALS

Mechanical forces are the integral determinants in cell and tissue homeostasis and regeneration, and they can affect numerous biological process from proliferation to fate determination. Mechanical forces that possess low magnitude and high frequency characteristics are also known as low intensity vibrations (LIVs). These signals were studied widely on many cell types for regenerative purposes, however most of these studies select components of LIV signals (e.g. magnitude, frequency, duration, etc.) arbitrarily. Here, we addressed the effect of LIV applied frequency, LIV daily exposure time and fate induction on the viability of preadipocyte 3T3-L1 cells. For this, we performed a frequency sweep that was ranging from 30 to 120 Hz with 15 Hz increments applied for 5, 10 or 20 minutes during quiescent growth or adipogenesis for up to 10 days. Results suggest that the applied frequency and fate induction was an important determinant of cell viability, lipid droplet physiology, triglyceride concentration, cell density and adipogenic-specific gene expression while daily exposure time had no effect. These findings contribute to the effort of optimizing a relevant mechanical stimulus that can inhibit adipogenesis.

On the other hand, random and aligned PAN/PPy nanofibers were investigated as a scaffold material for osteogenic differentiation of D1 ORL UVA mouse bone marrow mesenchymal stem cells. Cells were able to attach and grow on nanofibers confirmed by cell viability results. Stem cells that were cultured with osteogenic induction were able to mineralize on electrospun nanofibers based on alizarin red and Von Kossa dye staining. For aligned PPy nanofibers, mineralization occurred in the fiber alignment direction. Consequently, PAN/PPy nanofibrous mats in both random and aligned forms would be potential candidates for bone tissue engineering.

ÖZET

KEMİK İLİĞİ ÖNCÜL MEZENKİMAL HÜCRELERİNİN KİMYASAL VE FİZİKSEL UYARILARA KARŞI GÖSTERDİĞİ MOLEKÜLER VE HÜCRESEL ADAPTASYONLAR

Mekanik kuvvetler, hücre ve doku homeostazında ve rejenerasyonunda ayrılmaz belirleyicilerdir ve proliferasyondan farklılaşma sonucunun belirlenmesine kadar birçok biyolojik süreci etkileyebilir. Düşük yoğunluk ve yüksek frekans özelliklerine sahip mekanik kuvvetler, düşük yoğunluklu titreşimler (DYT'ler) olarak da bilinir. Bu sinyaller, rejeneratif amaçlar için birçok hücre türü üzerinde geniş çapta incelenmiştir, ancak bu çalışmaların çoğu, DYT sinyallerinin bileşenlerini (örneğin; yoğunluk, frekans, süre, vb.) keyfi olarak seçmektedir. Bu tezde, uygulanan frekansın, günlük DYT maruziyet süresinin ve farklılaşma indüksiyonunun preadiposit 3T3-L1 hücrelerinin canlılığı ve farklılaşması üzerindeki etkisine değindik. Bunun için, 10 güne kadar normal büyüme veya adipogenez sırasında 5, 10 veya 20 dakika süreyle uygulanan 15 Hz'lik artışlarla 30 ila 120 Hz arasında değişen bir frekans taraması gerçekleştirdik. Sonuçlar, uygulanan frekansın ve adipojenik indüksiyonunun hücre canlılığı, lipid damlacık fizyolojisi, trigliserit konsantrasyonu, hücre yoğunluğu ve adipojenik spesifik gen ekspresyonunun önemli bir belirleyicisi olduğunu ancak günlük maruz kalma süresinin hiçbir etkisi olmadığını göstermektedir. Bu bulgular, adipogenezi inhibe edebilecek mekanik bir uyaranı optimize etme çabasına katkıda bulunur.

Öte yandan, D1 ORL UVA fare kemik iliği mezenkimal kök hücrelerinin osteojenik farklılaşması için bir iskele malzemesi olarak rastgele ve hizalanmış PAN / PPy nanofiberleri araştırıldı. Hücreler, hücre canlılığı sonuçlarıyla onaylandığı üzere nanoliflere bağlanıp büyüyebildiler. Osteojenik indüksiyonla kültürlenen kök hücreler, alizarin kırmızısı ve Von Kossa boyamasıyla elektrospun nanofiberler üzerinde mineralizasyon oluşturabildiği gösterildi. Hizalanmış PPy nanolifler için, fiber hizalama yönünde mineralleşme meydana geldi. Sonuç olarak, hem rasgele hem de hizalı formlarda PAN / PPy nanofibroz matlar, kemik dokusu mühendisliği için potansiyel adaylar olacaktır.

Dedicated to my mom and dad…

TABLE OF CONTENTS

LIST OF TABLES

LIST OF FIGURES

Figure **Page**

Figure **Page**

CHAPTER 1

BACKGROUND AND SIGNIFICANCE

1.1. Bone Tissue, Structure and Function

Bone is a composite tissue as involving different organic and inorganic compounds in its structure like collagen, calcium phosphate, water, magnesium, sodium and bicarbonate [1]. The protein content of bone includes sialoprotein, osteonectin, osteocalcin and osteopontin providing arrangement and size of the crystal structure of minerals [2]. Moreover, there are small amounts of hydrogen phosphate, sodium, magnesium, citrate, potassium and carbonate ions in bone mineral [1, 3].

Bone is composed of two structure that are cortical (compact) and trabecular (spongy/cancellous) bone. Cortical bone is more dense and ordered compared to trabecular bone. The diaphyseal ends of the bone contain compact bone whereas epiphysial ends have spongy bone. Inner side of the compact bone contains the bone marrow (Fig. 1.1). Spongy bone is biologically more active than cortical bone. Bone remodeling occurs in the trabecular bone more often [4, 5].

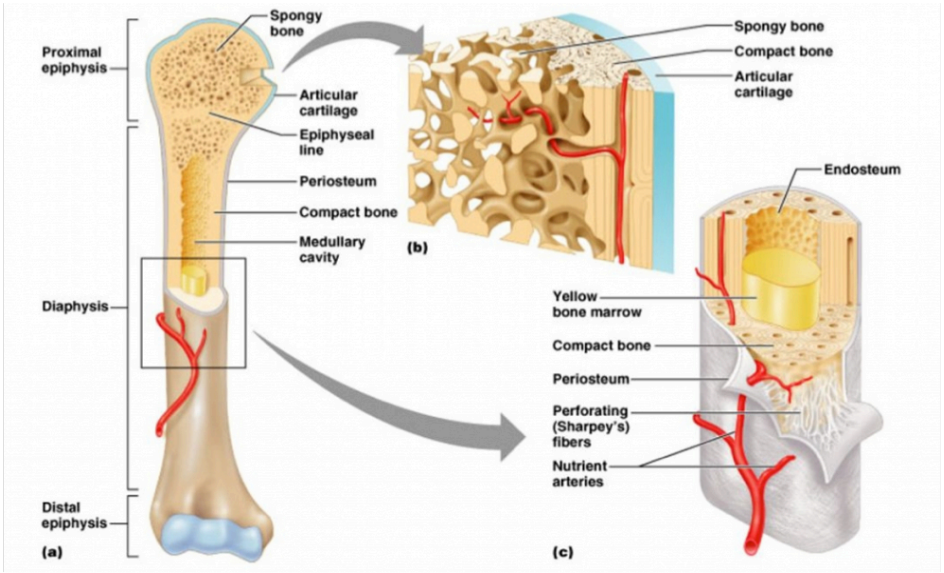

Figure 1. 1 Structure of a long bone (Copyright © 2004 Pearson Education, Inc., publishing as Benjamin Cummings)

Bone serves several functions in the body: (i) provides mechanical and structural support as a framework, (ii) helps the movement of the body together with tendons, muscles, joints and ligaments, (iii) acts as a buffer against to change in pH by storing calcium and phosphate needed for the maintenance of serum homeostasis, (iv) takes role in production of blood cells through the marrow, (v) protects internal organs such as brain, heart and lungs [6, 7].

Bone is composed of two cell types that are osteoblasts and osteoclasts carrying out bone formation and bone resorption events respectively leading to bone remodeling concept. Osteoblasts are uninuclear cells that generate non-calcified structure, osteoid that is mainly composed of matrix proteins and proteoglycans such as osteocalcin, osteopontin and bone sialoprotein, and polysaccharides as chondroitin sulphate, and water, by secreting collagen I protein content. Some of the osteoblasts become flat shaped and form lining cells that cover the outer surface of the bone. These lining cells are highly interconnected with the osteocytes in the bone matrix through a network of canaliculi [4, 5].

Osteocytes are mature bone cells having extensions that maintain the communication with each other and with lining cells. They also secrete growth factors, prostaglandins and nitric oxide that activate the lining cells and the osteoblasts [4, 5, 8].

Osteoclast cells are large multinucleated cells formed by fusion of mononucleated precursor cells like macrophages [9]. They attach to the bone tissue matrix; acidifies the microenvironment and dissolves the organic and inorganic matrices of the bone resulting in the bone resorption, osteolysis [8].

1.2. Mechanical Signals and Bone Tissue

Bone is actively dynamic organ and its function depends on mechanical forces such as gravity, blood pressure and muscle strains [10-19]. As a result of this, bone remodeling can also be regulated locally or systematically by external mechanical forces. A tennis player having a stronger bone on his actively playing arm is an example of local regulation while astronauts suffering from bone loss due to lack of gravity is a model for systemic regulation [20-22]. Thus, bone cells sense and respond to different forms of mechanical loads, including cyclic stretch [23], static pressure [24], shear stress [25, 26] and nanoscale mechanotransduction [27, 28].

Increasing bone mass through mechanical loads is an important biomedical aim, as these loads are natural and omnipresent for biological structures and they are

nonpharmaceutical in nature. For this aim to be achieved, however, individuals need to integrate planned physical activity into their daily routine. Unfortunately, that integration may not always be viable as individual compliance becomes an important hindrance [29, 30]. Furthermore, skeletal fragility in the elderly is another limiting factor for exercise to be employed for skeletal health. In order to trigger an adaptive response, mechanical loads should induce a level of strain (deformation normalized to geometry) on the bone structure. Magnitude of the strain is known to be a very important modulator for bone tissue [31, 32], but these high magnitude loads may cause fractures in the already frail skeletons of the elderly. Overall, utilization of mechanical loads to improve bone mass and morphology should overcome the problem of compliance and be safe to be applied to individuals.

Other than the peak strain magnitude of mechanical loads, several studies have concentrated on the frequency (number of loading events in a second) dependence of the anabolic response, based on the natural occurrence of high frequency yet low magnitude mechanical signals in the adult skeleton [33]. Indeed high frequency loads can trigger adaptive response in the skeleton even though their magnitude is far below mechanical loads that are experienced by the skeleton during daily activities [11]. In longitudinal studies, application of high frequency and low magnitude mechanical signals (referred to as low intensity vibrations (LIVs) hereafter) was found to be anabolic to bone tissue. LIVs provided significant benefits in bone mass by either increasing bone accrual or attenuating the bone loss in postmenopausal women [16], adolescent women [34], children with cerebral palsy [35, 36], adolescents with Down syndrome [37], and individuals with adolescent idiopathic sclerosis related osteopenia [38]. In contrast to strenuous physical activity or systemic pharmaceutical applications, application of LIVs is safe and natural for skeletal segments and triggering bone remodeling. On the other hand, application of LIVs may need to be optimized as its effectiveness may be limited as evidenced by other studies [39-41]. Therefore, the biological mechanisms on how LIV signals are perceived by bone and marrow cells is still a subject of biomedical research studies.

1.3. Cellular Response to LIV Signals

All tissue types in the human body are exposed to mechanical forces that differ and vary in applied mode, magnitude, duration and repetition. Taken broadly, physical modes of acting forces on tissues vary, for example cartilage tissue is mainly exposed to

compressive forces [42]; muscle [43] and tendons [44] work with tension; bone tissue is adapted to carry loads both in tension and compression [45], while blood vessels [46] and heart valves [47] mainly interact with fluid flow and experience hydrodynamic and shear forces [48]. Physiological and morphological effects of mechanical forces on organs and tissues were found to be related to all aspects of acting forces, including magnitude [49], rate and cycle number [50], frequency [11, 14, 51-54], duration [55], and load distribution [56]. However, cellular level determinants of sensation and response to mechanical signals remain largely unknown.

The effect of mechanical stimulation of biological components at different organizational levels has been studied for a long time by the application of pseudo physiological stimulation with various techniques such as micropipette aspiration [57], hydrostatic pressure [58] and fluid shear [59]. A specific subgroup of mechanical loading regimens can be categorized as Low-Intensity Vibrations (LIV), which implies vibratory (repetitive) loading with low magnitudes and high frequencies. Studies suggest that LIV not only offer insight on how cells can sense and respond to physical loads but also can be used as an alternative to biochemical and scaffold induced signals or in combination with them to regulate cellular behavior and differentiation.

1.4. Description of Mechanical Signals in Biomedical Applications

Low-intensity vibrations are mechanical signals that have small magnitude and high frequencies. This loading strategy is also named as Low Magnitude Mechanical Stimulation [11, 60], Low Magnitude Mechanical Signals [61], High-Frequency Oscillatory Motions [62], Low Magnitude Vibrations [12], Low Level Vibrations [15] and Mechanical Vibrations [63] in the literature. The magnitude (or amplitude) is considered as small (low-intensity) when it is lower than the earth's gravitational field ($g=9.81 m/s^2$). The frequency of the signal corresponds to the number of repeats, generally reported as per second (Hz) for a given duration [64]. There are also examples of applied mechanical signals to be reported as: sub-sonic vibrations, with frequency values lower than 20 Hz [65], micro-vibrations, which are generally applied in 5 sec/60 min cycles [66-68], and nano-vibrations with nanoscale displacement values such as 1 to 4 nm [69].

1.5. Stem and Progenitor Cells

Stem cells are unique cell types that have the ability of self-renewal and capacity for differentiation into somatic cells [70]. Totipotent stem cells (for example zygote) are able to differentiate into whole organism while their differentiation potency is reduced as they specialize. On the other hand, pluripotent stem cells, such as embryonic stem cells, can differentiate into three germ layers but not the whole organism [71]. Adult stem cells are multipotent stem cells that can differentiate into one germ layer such as mesenchymal stem cells which can differentiate into mesoderm-type cells, osteocytes, adipocytes and chondrocytes [72]. Stem cell research is utilized extensively in biomedical science and engineering for microfluidic studies [73, 74], regenerative medicine [75], biomaterial design [76] and biomechanics [77].

1.6. Application of Low-Intensity Vibrations on Stem Cells

Stem cells can be collected from various tissue-specific sources depending on the performed study and the aim.

1.6.1. Bone Marrow-derived Stem Cells

Mesenchymal stem cells are commonly isolated from bone marrow based on their adherence to the substrate and subsequent proliferation [78]. Bone marrow-derived stem cells became important sources for their usage for the treatment of many diseases [79] and tissue engineering to heal damaged tissue and organs [80]. Application of LIV on bone marrow-derived MSCs mainly focused on proliferation and stem cell lineage selection behavior.

D1-ORL-UVA cells (ATCC-CRL-12424) are mouse multipotent adult mesenchymal stem cells that are able to differentiate into osteocytes, chondrocytes and adipocytes in the presence of the appropriate stimulus and environment. Daily application of LIV (0.1g, 90 Hz, 15 min/day) for 7 days regressed the adipogenesis of D1-ORL-UVA cells induced by chemical factors by decreasing the expression of adipogenic genes [81]. In addition, it resulted in alterations on cell morphology through regulation of actin cytoskeleton leading suppression of rounded cells that are hallmark characteristics of adipogenic commitment [82]. Furthermore, application of LIV during adipogenic induction

reduced the plasticity of stem cells for commitment to osteogenesis once the adipogenic induction was changed to osteogenic induction. The induction of osteogenesis in LIV applied D1-ORL-UVA cells was explained in another study that applied the same loading regimen, resulting in the increased actin content, actin fiber thickness and the cell height in all LIV applied cells and upregulation of Runx2 and focal adhesion kinase (FAK) expression, for cells that were cultured in osteogenic environment [83].

In another study with a higher magnitude (0.3g) and lower frequency (40 Hz) and longer duration (30 min) LIV signals, bone-marrow derived mesenchymal stem cells (BMSCs) harvested from Sprague-Dawley rats and grown on hydroxyapatite-coated surfaces had an increase in fibronectin levels and remodeling of actin cytoskeleton with upregulation of β1 integrin, vinculin and paxillin mRNA levels after 14 days [84]. In contrast to the previous example of the anti-adipogenic effect of LIV, the same loading regimen increased the expression of adipogenic mRNA markers and lipid droplet accumulation on BMSCs under adipogenic conditions [85]. When cell viability is considered, the same loading protocol (0.3g and 40 Hz) applied on BMSCs, increased proliferation of cells that are in growth medium but decreased proliferation of cells in the osteogenic medium [86]. However, when human BMSCs isolated from healthy donors were exposed to 0.3g, 30 to 40 Hz for 10 min/day for 5 days, they showed increased proliferation with increased mineralization and alkaline phosphatase (ALPase) activity [87]. In a similar magnitude (0.3g) but varying frequency (30, 400 and 800 Hz) LIV application for 30min/day, human BMSCs showed increased cell proliferation at day 7 and expressions of osteogenic specific genes at day 14 with 800 Hz while the expression of adipogenic genes was decreased at day 21 with 800 Hz [88]. However, 30 Hz vibrations decreased osteogenesis evidenced by decreased mineralization at day 14 under adipogenic conditions, revealing that the same signal magnitude resulted in the different fate selection outcomes based on the frequency.

In studies that used higher magnitude LIV signals, human BMSCs showed decreased proliferation rate but increased ALP and Runx2 gene expressions when exposed to 0.6g, 30 Hz vibrations for 45 min/day during 3-6 weeks [89]. Another high magnitude vibrations study applied on human MSCs with 25 Hz and 14g mechanical signals, resulted in increased CD29 and CD44 expression of cells, which are considered as mesenchymal cell markers, and decreased cell number and viability [90], establishing the anti-proliferative effect of higher acceleration (g) values.

1.6.2. Adipose-derived Stem Cells (ADSCs/ASCs)

Adult mesenchymal stem cells can also be isolated from subcutaneous adipose tissue depots, which can clinically be obtained through liposuction applications. A large amount of tissue is obtained through these surgeries and this material is generally discarded if not used [91]. ADSCs also show the stem cell-specific combination of surface markers similar to MSCs isolated from bone marrow, such as CD90, CD105, CD73, CD44 and CD166 [92].

In a LIV application on human ASCs for 21 days for 10 min/day with 0.3g and 25, 35 and 45Hz signals, increased osteogenic differentiation capability and cell proliferation activity was observed with 25 Hz signal being optimal for osteogenic induction with the highest expression of osteocalcin (OCN) and osteopontin (OPN) mRNA [93]. In a similar study with matching signals applied for 15min/day, LIV signals were found to suppress the adipogenic capacity and increase the chondrogenic capacity of ADSCs with 35 Hz signal being the optimal frequency for cartilage tissue formation with increased BMP-2 and Collagen Type 2 secretion [94].

On the other hand, when the magnitude of the prescribed acceleration was significantly higher as 3g, 50 and 100 Hz frequency-vibrations for 3h/day for 14 days induced the osteogenic differentiation of human ASCs with increased ALPase activity, collagen production and mineralization without any significant change at cell number and viability at both frequencies [95]. Inhibited adipogenesis was also observed in this study with decreased lipid accumulation within the cells. In another experiment, human ASCs cultured for 28 days at daily 30 Hz vibrations (acceleration not reported) applied for 40 min/day, showed increased mineralization in both osteogenic and growth conditions [96]. Also, mRNA expression level of osteogenic genes such as Collagen Type 1, OPN and ALP was increased by vibrational signals.

Aside from implications of LIV in bone regeneration, sub-sonic vibrations applied with 1.0V at 10, 20, 30 and 40 Hz frequencies on adipose tissue-derived MSCs for 4 days led to induced neurogenesis by increased expression of MBP, GFAP, NF-L, NeuroD1 and Nkx22 genes in addition to the increased neural antibodies [97]. This study concluded that 30 Hz is the most effective frequency value not only for inducing neural differentiation but also inhibiting adipogenesis in ADSCs.

1.6.3. Embryonic Stem Cells

Even though ethical concerns and accessibility largely restrict studies with embryonic stem cells (ESCs), it is still possible to encounter studies with the application of vibrational loads on cells derived from ESCs. Stem cells collected from the umbilical cord of infants born through Cesarean section responds to subsonic vibrations of 1.0V and 10, 20, 30 or 40 Hz frequency for 5 days by increased expression of MAP2, NF-L and NeuroD1, indicating the neurogenic effect of mechanical stimulation similar to ADSCs [98]. Researchers concluded that neurogenesis was sustained through a time-dependent increase in levels of ERK molecule in response to vibrations. In another study, embryonic derived MSCs were subjected to 15, 30, 45 and 60 Hz of 0.2m/s^2 (0.02g) vibrations for 10 or 45 min for 1-2 days to test if their osteogenic potential is augmented and results suggested that 60 Hz signals induced highest ALP activity if the osteogenic culture was supplemented with dexamethasone [99].

1.6.4. Progenitor cells

Progenitor cells do not have the ability for self-renewal and they are generally unipotent in their commitment that they can differentiate into only one cell type [100]. However, the plasticity of progenitor cells in cell culture is challenging to assess, as some cells may retain the ability to commit to another lineage. For example, bone marrow-derived D1 ORL UVA cells were able to mineralize once their adipogenic induction was switched to osteogenic induction and daily 0.1 g and 90 Hz LIV signals increased number of nodules and size that mineralize [81]. Another study, unlike previously described stem cell-based results, showed the application of 0.5V, 20 and 30 Hz vibrations inhibited the proliferation and increased the adipogenesis of 3T3-L1 preadipocyte progenitors when applied for 6 days with increases in cellular triglyceride content and mRNA upregulation of adipogenic signature genes of PPARγ and cEBPα [101]. In another study, 0.5g, 45 Hz vibrations for 1 hour/day for 3 days increased the osteoblastic proliferation and matrix mineralization of rabbit calvaria harvested cells through modulation of Wnt signaling [102]. The study with 3T3-E1 preosteoblast progenitor cells (with 40 Hz-vibration at different magnitudes (0.06, 0.14, 0.32, 0.49, 0.66 or 0.8g) for 30 min/day for 3 days showed the greatest increase in BMP2 and Osterix mRNA expressions at 0.49g while the highest Runx2 protein was obtained at 0.32g [103]. On the other hand, application of 1.0-10m/s^2

(0.1g-1g) acceleration and 30, 60 and 90 Hz vibration on 3T3-E1 cells for 10 min revealed that 5.0m/s^2 (0.5g) and 60 Hz combination was the best condition for osteogenesis by increased Runx2, Osterix and ALP mRNA levels [104].

Macrophages and monocytes as a model of progenitor cells for osteoclastic cells were also studied in the context of vibrational signals. Four combinations of 0.15g and 0.1g with 30 Hz and 100 Hz vibrations on murine macrophages for 3 days, twice a day for 20 min after 2h of resting resulted in an increase of macrophage number with a suppression of their inflammatory properties indicated by decreased protein levels of IL-6, IFN-γ, and TNF-α, and induction of mRNA expression of pro-healing factors such as VEGF and TGF-β [105]. In a contrast in applied frequency, it was previously noted that low frequency dynamic loads increase mRNA expression of osteoclast marker genes in cells of hematopoietic origin [106].

Taken together with reports from stem cells, mechanical stimulation in high frequency vibratory form induce osteogenesis and suppress adipogenesis in stem and progenitor cells. Viability results on the other hand suggest that for proliferation cells may either ignore low intensity vibratory stimulus or increase proliferation, but never show reduced numbers.

1.6.5. Human Periodontal Ligament Cells (HPDLC) and Vibration

Another type of cells that are commonly used as a source for osteogenic differentiation and vibration studies are human periodontal ligament cells which are shown to be a promising therapy for the regeneration of damaged periodontal tissue by several preclinical trials [107], potentially containing a pool of stem and progenitor cells [108]. In a study that applied LIV to HPDLCs at 0.3g with 30, 60 and 90 Hz frequencies for 20 min/day, researchers reported increased osteogenic gene expressions as early as 48 hours [109]. Moreover, 0.05g to 0.9g with 50 Hz LIV for 30 min increased HPDLC mRNA expression of ALP, OCN, Collagen Type 1 and Runx2 with thicker F-actin stress fibers compared to control cells [110]. Similarly, low frequency cyclic stretching with 0.1 Hz for 6, 12 and 24 hours upregulated the Runx2, ALP and OCN protein expression levels in HPDLC [111]. In another study, 0.3g magnitude 10 to 180 Hz frequency, 30 min/day LIV application increased the ALPase activity in a frequency-dependent manner that reached the highest level at 50 Hz with the significant increase in Collagen Type 1, osterix and Runx2 mRNA expression. Moreover, OCN mRNA level was increased at 40, 50, 60, 90

and 120 Hz frequencies while Collagen Type 1, osterix and Runx2 mRNAs were only higher at 40 and 50 Hz [112]. On the other hand, the proliferation of the cells was lower in vibration groups compared to control. Another report on cyclic tensile strain applied to HPDLC at 3000 microstrain for 3, 6, 12 and 24 h raised the protein and gene expression levels of osteogenic markers in the non-osteogenic culture medium [113].

1.7. Molecular Level Acting Mechanism of Vibrations

Although the exact mechanisms of how the mechanical signals are transmitted and processed within the cells is not fully understood, some studies reveal a few key point elements taking a role in this mechanotransduction event. One of the studies performed showed that 0.7 g, 90 Hz vibrations and uniform 2% equibiaxial strain at 10 cycles per minute that are both for 20 min twice a day with a 2h-resting period decreased the nuclear β-catenin level but its interaction with the nucleoskeleton increased. It is also suggested that this dynamic action of β-catenin is provided by the Linker of Cytoskeleton and Nucleoskeleton Complexes (LINCs) elements like Sun-1 and Sun-2 [114]. In other words, forces acting on integrins such as vibratory signals are delivered from actin cytoskeleton to LINC and then upregulate the transcription via chromatin stretch through the lamina-chromatin interactions [115]. Additionally, another study stated that biaxial cyclic mechanical strain of 0.1%-10%-Hz on human multipotent/stem progenitor cells (EPCs) led to the replacement of H3K9me2,3 with H3K27me3 through the mechanosensory complex of emerin (Emd) which acts as a nuclear force sensor [116]. Cytoskeleton and nucleus integration is also accompanied by the activation of focal adhesion kinases (FAK) and Akt signaling followed by FAK-dependent induction of RhoA in MSCs after 90 Hz and 0.7g vibration for 20 min [117].

C3H10T1/2 embryonic MSCs exposed to 0.7g and 90 Hz vibratory signals showed decreased adipogenesis through the β-catenin involved process [118]. It was shown that Wnt signaling takes a role in the mechanotransduction of 3T3-E1 preoteoblast cells subjected to 0.06, 0,14, 0.32, 0.49, 0.66 and 0.8g magnitude vibrations with 40 Hz frequency for 30 min per day for 3 days [119]. In addition to all of these molecules acting in the mechanotransduction, another study demonstrated that phosphorylation of p38 MAPK was enhanced by the 0.3g, 40 Hz vibrations for 15 min on MSCs at day 1, 4 and 8 [120].

CHAPTER 2

APPLIED FREQUENCY BUT NOT THE EXPOSURE TIME OF LOW INTENSITY VIBRATIONS INFLUENCE CELL VIABILITY 3T3-L1 CELL DURING ADIPOGENESIS

2.1 Mechanical Signals and Effect on Cell Viability

Mechanical forces are relevant and integrated factors involved in all biological processes [121, 122]. Cells may be developmentally specialized to work under a dominant load settings (such as compressive, tensile or shear loads) based on their function, however all cells, irrespective of their physiological specialization, are constantly subjected to a barrage of internal and external mechanical forces naturally and these forces can influence an organism related to development to maintenance and repair [123-126]. Mechanical loads that a cell experience continuously can be identified and categorized based on their magnitude and their repetition per time frame (frequency). Natural forces occurring across the body can be in high magnitude and low frequency in daily activities such as walking and running [127]. However, some of the natural forces can also act in high frequencies (>30 Hz) with very low magnitudes that are smaller compared to forces generated by Earth's gravitational field [33, 125].

Since mechanical loads are implicated as regulatory factors for healthy tissues and organs [128] methods that aim to generate and deliver biomimetic mechanical signals to tissues of interest have important biomedical relevance especially for regenerative medicine [125, 129-132]. Low intensity vibrations (LIVs) can be exogenously applied as noninvasive biophysical signals [133]. Unlike physical exercise, LIV treatment has high compliance among subjects patients [134] with a low risk of inducing mechanical failure in the skeleton [16, 135]. With this prospect, LIV treatment has been tested in clinical studies with varying degrees of success in bone and bone marrow health. In a study on postmenopausal women, significant increase in bone mineral density was reported with LIV treatment (0.2g, 30 Hz, up to 20 min/day for one year) [52], as well as LIVs with 0.2g, 30 Hz 2/d for one year [16, 133]. Similarly, (30 Hz, 0.3g) LIVs applied to 48 young women (10min/d during 12 months), showed increased bone mineral density (BMD) and bone area [135]. Adolescent females that have reduced skeletal quality due to bed rest and

anorexia nervosa showed increased bone turnover as a response to LIV treatment (0.3 g, 32-37 Hz, 10 min/ day for 5 days) [136]. Finally, LIV treatment (0.3g, 30 Hz, 12 months) was found to increase the bone mineral density of young women with osteopenia while suppressing adipogenesis significantly [137].

As LIV treatment appear to be anabolic for bone tissue, yet suppressive for adipose tissue in the rodent models and the clinic [15, 138-140], numerous studies were designed to elucidate how bone osteoprogenitor / stem cells sense and respond to LIV signals in vitro [141]. Applied to bone marrow stem cells, LIV signals (0.1g, 90 Hz, 15min/day for 3weeks) increased cell proliferation, mineralization and induced an increase in mRNA expressions for osteogenic markers with cytoskeletal adaptations [83]. Similarly, LIV signals (0.5g, 30 Hz, 45 min/ day – 3–6 weeks) increased osteogenic mRNA markers such as Runx2 and enhanced calcification in primary bone marrow cells [142]. In other study LIV signals (0.1g, 90 Hz, 15 min/day for 21 days) applied to MSCs on a 3D cell culture model increased the osteocalcin expression and extracellular matrix formation [143]. Similarly, LIV (0.3g, 30–40 Hz, 10 min/day – 1–3 weeks) increased mineralization and osteogenic mRNAs such as osteocalcin, osteopontin, and bone sialoprotein when applied to cells in 3D culture conditions [87]. In addition to the primary bone marrow cells, adipose tissue derived stem cells cultured under osteogenic culture conditions respond to LIV signals (30 Hz, 45 min – 4 weeks) and significantly increased calcification and expression of osteogenic genes such as osteopontin, alkaline phosphatase, and collagen type I [132]. In parallel to in vitro studies related to osteogenesis, the effects of LIV signals during the adipogenic differentiation of bone marrow stem/progenitor cells are also studied for potential mechanisms. LIV application (0.1g, 90 Hz, 15min/d) during one week normalized the adipogenesis-induced changes on bone marrow MSCs where expression levels of PPARγ, C/EBPα, adipsin and resistin were decreased and decreased viability of MSCs during adipogenesis was rescued [144]. Moreover, the lipid droplet formation under adipogenic differentiation conditions was suppressed in the vibration-stimulated hASCs at the 14 day time point after 3g, 50 or 100 Hz for 1.5 h vibration [95]. LIV regimen (0.7 g, 90 Hz) which was divided into 2x20min bouts separated by 41h, resulted in PPARγ and adipocyte protein 2 decrease and prevented the lipid droplet formation of MSCs [118]. Though a plethora of studies showed vibratory stimulus is effective in inducing biological response on cells of mesenchymal origin, loading parameters drastically vary for the amplitude, frequency, and duration between different studies. Therefore, a complete understanding of how LIVs govern

biological response requires unified study designs that will test the effect of separate parameters related to the biological goal of interest.

In this study, we aimed to understand frequency- and exposure duration-dependent effects of LIV signals on the bone marrow preadipocyte viability in vitro. Preadipocytic 3T3-L1 cells that were cultured in either quiescent growth or adipogenesis media were exposed to a LIV frequency sweep ranging from 30 to 120 Hz, with applied durations of 5, 10 or 20 minutes/day. Viability data was assessed at selected time points between 1 to 10 days. Results indicate that in terms of viability, preadipocytic bone marrow cells were affected by adipogenic induction and applied frequency, but not the exposure duration time of LIV stimulation.

2.2 Methods

2.2.1 Cell Culture and Adipogenic Induction

3T3-L1 (ATCC CL-173) mouse embryo fibroblast cells were cultured in Dulbecco's Modified Eagle's Medium (Gibco, Ref#11320-074) with 10% new born calf serum (NBCS) (Biological Industries, Cat#716684) and 1% penicillin/streptomycin (Invitrogen, Cat#1092595) at 37ºC, 5% CO2. Cells were passaged with 0.25% trypsin/EDTA solution (Biological Industries, Cat# 03-052-1B) at 37 °C, 5% CO2 for 5 min incubation before 1.2 rpm centrifugation for 5 min. 2 days after seeding of 3T3-L1 cells in plate, adipogenic induction was started by adding 5 µg/ml of insulin from bovine pancreas (Sigma, Lot#SLBD3067V), 10 nM of dexamethasone (Sigma, Lot#BCBK1265V) and 50 µM of indomethacine (Sigma, Lot#BCBF9122V) into growth medium. Cells were cultured at 37ºC, 5% CO2 after starting the induction.

2.2.2 Application of Low Intensity Vibration (LIV) Signals

Mechanical signals were applied in vitro as previously described using vibrating platform as previously described [60, 83, 144]. Low intensity vibration (LIV) signals were applied at 0.1g but varied in frequency as 30Hz, 45Hz, 60Hz, 75Hz, 90Hz, 105Hz and 120Hz between subjects tuned using a software interface via MatLab. Furthermore LIV exposure time was varied as 5min, 10min and 20min/day between subjects. Cells

received LIV signals up to 10 days under ambient conditions, while control groups received a sham treatment simultaneously.

2.2.3 Determination of Adipogenic Differentiation of 3T3-L1 Cells

Lipid accumulation was detected by Oil-red-O staining. Cells were washed with 0.5 ml of 1× PBS (×2) and fixed with 0.5 ml of 10% Neutral Buffered Formalin for 15 min at room temperature. Later, cells were rinsed with 0.5 ml of dH2O (×2) and stained with 0.5ml of 60% diluted 0.5% Oil-red-O in isopropanol (Amresco, Lot#1291C081) for 45 min at 37^{o}C. Cells were rinsed with 0.5 ml of dH2O (×3). Stained samples were visualized by an inverted microscope (Olympus, IX-83).

2.2.4 Determination of Cell Viability

The effect of external mechanical signals and adipogenic induction on the viability of 3T3-L1 cells was tested by MTT (3-(4,5- Dimethylthiazol-2-yl)-2,5-Diphenyltetrazolium Bromide) assay. Cells were seeded at a density of 250 cells per well in 24 well plates. 2 days later, mechanical signal application and adipogenic induction was initiated based on the experimental group. MTT assay was applied on Day 1, 3, 5, 8 and 10 by adding 600 µl of 10% MTT solution (5mg/ml in 1× PBS, (Amresco LLC, USA)) in growth medium. The cells were incubated for 4 h at 37°C. The formazan crystals, which were formed, were then solubilized in DMSO (600 µl/well) by pipetting and transferred to 96-well plate in triplicates (200 µl/well). The cell viability was measured by VarioScan spectrophotometer at 570 and 650 nm wavelength at Day 1, 3, 8 and 10.

2.2.5 Statistical Analyses

All results were presented as means ± standard deviation. Cell viability data was normalized from different LIV applications were normalized twice, 1) to corresponding sham controls of same batch and then 2) viability data at day 1 of the same batch. Significant effects and significant interactions of exposure time, applied frequency, and induction on viability were determined using generalized linear models (JASP Version 0.13.1). Multiple comparisons of grouped data was performed by ANOVA followed by

Tukey test, where p values smaller than 5% was accepted as an indicator of significant difference.

2.3 Results

3T3-L1 cells that were subjected to growth or adipogenic induction for up to 10 days and at the end of the process rounding and lipid accumulation was clearly visible in adipogenic group while control cells retained their fibroblastic morphology (Figure 2. 1). Cell viability was tested after application of varying parameters of LIV signals. Viability data was presented as a fold-increase of corresponding sample compared to its Day 1 value at different time points, and then further normalized to the fold increase of corresponding control cells that were measured for every condition and replicate (Figure 2. 2). According to the general results, cell viability of growth condition cells appeared to be inconsistently affected from variations of LIV frequency, while in adipogenic group 75 Hz signals consistently increased cell viability for all time points. Viability results were then used to set up a generalized linear model (GLM) to determine significant effects and interactions of parameters used in the study for different time points.

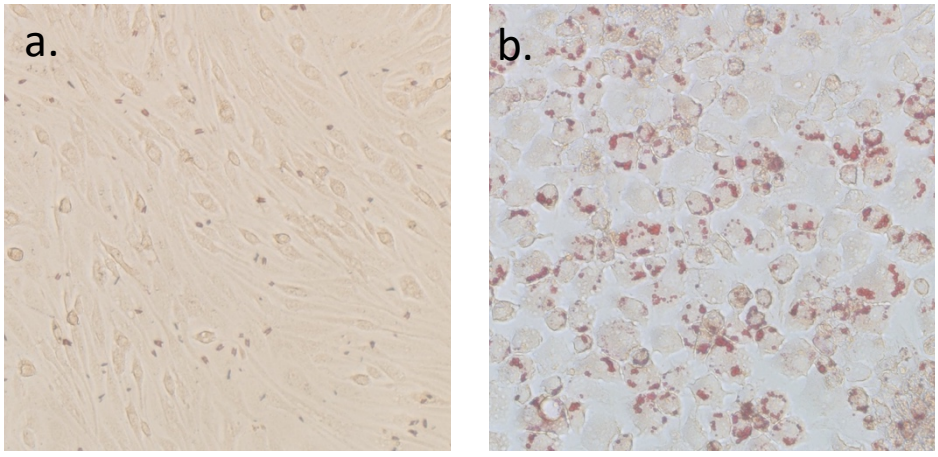

Figure 2. 1 Oil-red-o staining of the lipid structures of 3T3-L1 cells at day 10 with the growth control **(a)** and adipogenic control **(b)** groups at 20× magnification.

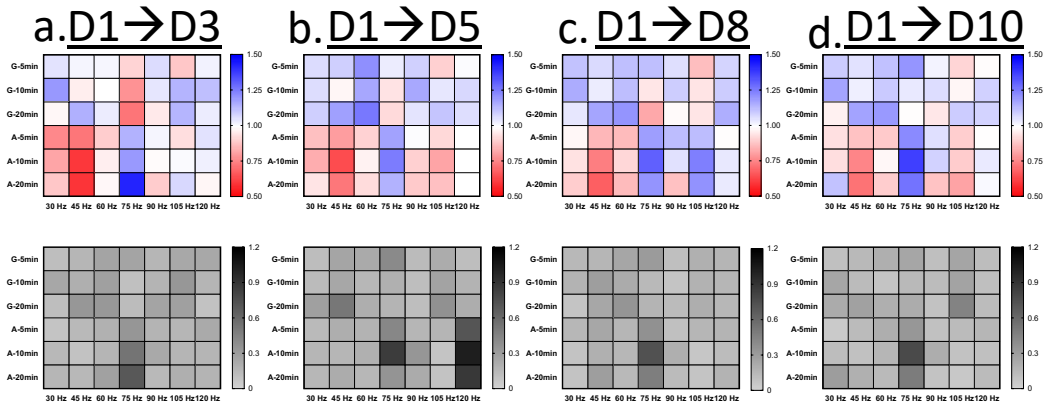

Figure 2. 2 Heatmaps demonstrating the normalized change in cell viability average (blue-white-red) and standard deviation (greyscale) values on **(a)** at 3 days; **(b)** at 5 days; **(c)** at 8 days and **(d)** at 10 days. Rows represent daily exposure duration and induction, while columns represent the applied frequency.

Table 2. 2 Generalized linear model output (type III sum of squares) of normalized viability results modeled with; LIV exposure duration (5 min/day, 10 min/day or 20 min/day); LIV applied frequency (30 Hz, 45 Hz, 60 Hz, 75 Hz, 90 Hz, 105 Hz or 120 Hz); induction media (growth or adipogenic) as fixed factors. Columns corresponds to different experimental time points. Statistically significant (<5%) factors or interactions were depicted as bold.

		D1→D3	**D1→D5**	**D1→D8**	**D1→D10**
Cases	***df***	***p***	***p***	***p***	***p***
Exposure Duration	2	0.661	0.894	0.478	0.754
Applied Frequency	6	**< .001**	**< .001**	0.064	**< .001**
Induction	1	**0.021**	0.260	0.085	**0.006**
Duration × Frequency	12	0.373	0.974	0.713	0.919
Duration × Induction	2	0.578	0.878	0.681	0.775
Frequency × Induction	6	**< .001**	**< .001**	**< .001**	**< .001**
Duration × Frequency × Induction	12	0.271	0.994	0.750	0.230

At day 3 of the experiment, viability increase of 3T3-L1 cells were affected significantly from the applied frequency of LIV signal ($p<0.001$), adipogenic induction ($p=0.021$) as well as from the interaction between applied frequency and induction ($p<0.001$), but not exposure time or interactions including exposure time according to the GLM output (Table 2. 1). For averaged results of exposure time and applied frequency, cells that received adipogenic induction showed 6% ($p=0.021$) lower viability compared to cells that were cultured only in growth media (Figure 2. 3a). For averaged results of exposure time and induction, significant differences in applied frequency was observed between 45Hz and 75Hz (22% difference, $p=0.002$), 90Hz (18%, $p=0.031$), 105Hz (22%, $p=0.002$) and 120Hz (23%, $p=0.001$) but between no other groups (Figure 2. 3b). For averaged results of only exposure time, viability of 3T3 cells displayed significant differences based on applied frequency and induction interaction based on growth or adipogenic conditions (Figure 2. 3c and 2. 3d). For the viability of 3T3 cells in growth conditions, 75Hz group was significantly lower compared to 30Hz (25%, $p=0.04$), 105Hz (24%, $p=0.02$) and 120 Hz (24%, $p=0.02$) but no other groups showed any significant differences (Figure 2. 3c). For 3T3 cells that received adipogenic induction, cells that received 75Hz signals had cell viability significantly higher compared to 30Hz (53%, $p<0.001$), 45Hz (95%, $p<0.001$), 60Hz (33%, $p<0.001$), 90Hz (30%, $p=0.002$), 105Hz (25%, $p=0.017$) and 120Hz (23%, $p=0.036$) groups (Figure 2. 3d). Furthermore, for cells that received adipogenic induction there were significant differences in viability between 45Hz and 60Hz, 90Hz, 105Hz and 120 Hz (68%, 67%, 64%, 63%, respectively, all $p<0.001$). Finally, the differences between cell viability between growth and adipogenic conditions between different applied frequencies was significant at 30 Hz (31%, $p=0.017$); 45Hz (62%, $p<0.001$) and 75Hz (64%, $p<0.001$), but for no other applied frequency (Data analyzed in comparison of Figure 2. 3c and 2. 3d).

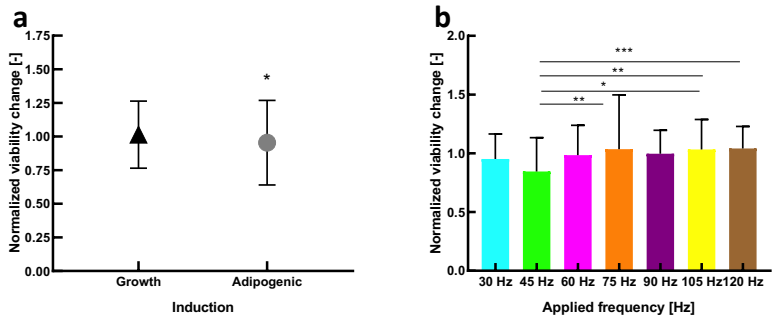

(cont.)

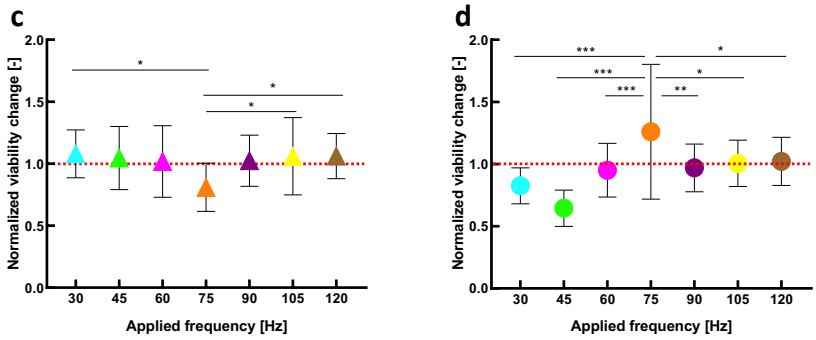

Figure 2. 3. Viability change of 3T3-L1 cells from day 1 to day 3 that is normalized to controls grouped based on **(a)** only induction media they received or **(b)** only applied frequency they received. Furthermore results were also represented for cells that **(c)** received growth induction grouped for applied frequency and **(d)** received growth induction grouped for applied frequency. Significant differences between groups were found by Tukey post-hoc tests and depicted with *:$p<0.05$, **:$p<0.001$ or ***:$p<0.001$. Red dashed line signifies the change of viability in corresponding controls.

At the day 5 of the experiment, viability change was affected significantly from the frequency of applied mechanical stimulation ($p<0.001$) and the interaction between applied frequency and induction ($p<0.001$) according to the GLM output (Table 2. 1). For averaged results of exposure time and applied frequency, cells that received adipogenic induction showed no significant difference in viability compared to cells that were cultured only in growth media in contrary to Day 3 (Figure 2. 4a). For averaged results of exposure time and induction, significantly higher cell viability was observed between 120 Hz and 30 Hz (39%, $p<0.001$), 45Hz (50%, $p<0.001$), 60Hz (26%, $p=0.001$), 75Hz (26%, $p=0.001$), 90 Hz (33%, $p<0.001$) and 105Hz (41%, $p<0.001$) but between no other groups (Figure 2. 4b). For averaged results of only exposure time, viability of 3T3 cells showed significant differences based on applied frequency and induction interaction (Figure 2. 4c and Figure 2. 4d). For the viability of 3T3 cells in growth conditions, there was no significant difference within the applied frequencies (Figure 2. 4c). However, for 3T3 cells that received adipogenic induction, cells that received 120Hz signals had significantly higher cell viability than 30Hz, 45Hz, 60Hz, 75Hz, 90Hz and 105Hz (89%, 130%, 78%, 40%, 79% and 92%, respectively, all $p<0.001$). Furthermore, for 3T3 cells

that received adipogenic induction, cells that received 75Hz signals had cell significantly higher cell viability than 45Hz (64%, $p<0.001$) (Figure 2. 4d). Finally, the differences between cell viability between growth and adipogenic conditions between different applied frequencies was significant at 45 Hz (49%, $p=0.019$) and 120 Hz (63%, $p<0.001$), but for no other applied frequency.

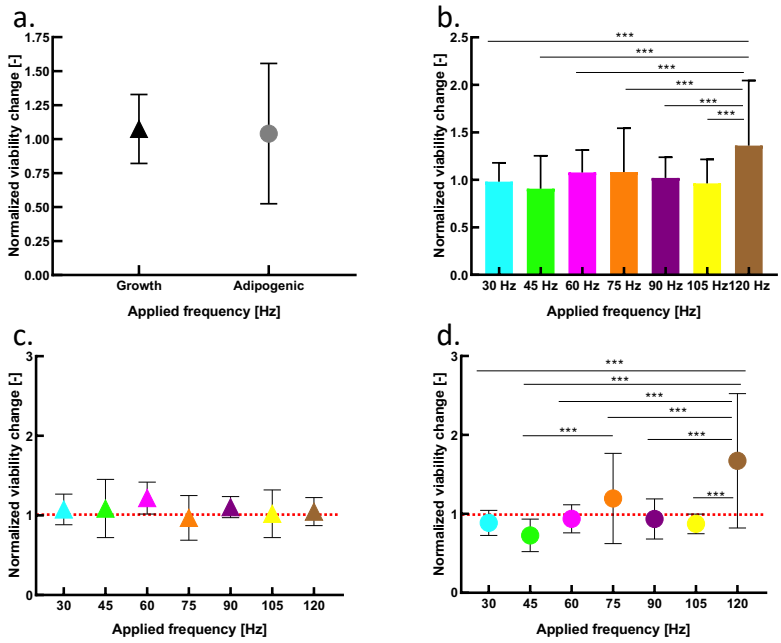

Figure 2. 4. Viability change of 3T3-L1 cells from day 1 to day 5 that is normalize to controls grouped based on **(a)** only induction media they received or **(b)** only applied frequency they received. Furthermore results were also represented for cells that **(c)** received growth induction grouped for applied frequency and **(d)** received growth induction grouped for applied frequency. Significant differences between groups were found by Tukey post-hoc tests and depicted with *:$p<0.05$, **:$p<0.001$ or ***:$p<0.001$. Red dashed line signifies the change of viability in corresponding controls.

At the day 8 of the experiment, viability change was affected significantly from the interaction between applied frequency and induction ($p<0.001$) according to the GLM output (Table 2. 1). For averaged results of exposure time and applied frequency, similar to the observation at day 5, cells that received adipogenic induction showed no significant difference in viability compared to cells that were cultured only in growth media (Figure 2. 5a). For averaged results of exposure time and induction, cells that received 75Hz

signals had 20% higher cell viability compared to 45Hz (p=0.02) (Figure 2. 5b). For averaged results of only exposure time, in growth conditions, there was no significant difference between applied frequencies (Figure 2. 5c). However, for the cells that received adipogenic induction, cells that received 75Hz signals had significantly higher cell viability than 30Hz, 45Hz and 60Hz (31%, 62% and 40% respectively, all p<0.001). Likewise, cells that received 105Hz signals under adipogenic induction had significantly higher cell viability than 30Hz (27%, p=0.039), 45Hz (57%, p<0.001) and 60Hz (36%, p=0.001). Furthermore, cells that received 90Hz signals under adipogenic induction had 34% higher cell viability than 45Hz (p=0.035) (Figure 2. 5d). Finally, the differences between cell viability between growth and adipogenic conditions between different applied frequencies was significant at 45 Hz (44%, p=0.005), 75Hz (78%, p=0.006) and 105Hz (77%, p=0.018), but for no other applied frequency.

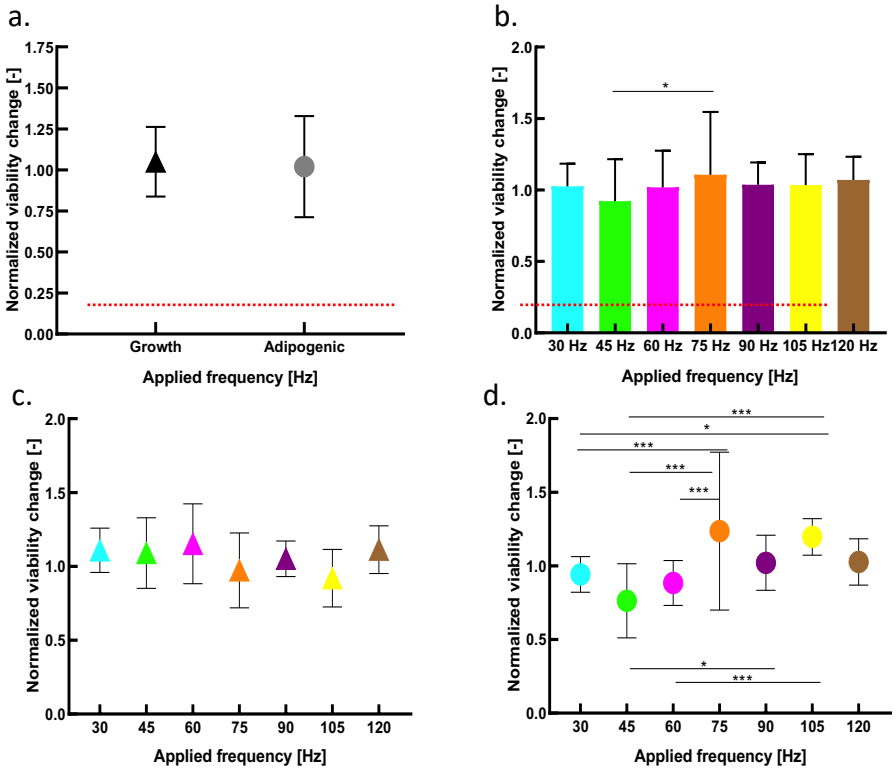

Figure 2. 5. Viability change of 3T3-L1 cells from day 1 to day 8 that is normalize to controls grouped based on **(a)** only induction media they received or **(b)** only applied frequency they received. Furthermore results were also represented for cells that **(c)** received growth induction grouped for applied frequency

and **(d)** received growth induction grouped for applied frequency. Significant differences between groups were found by Tukey post-hoc tests and depicted with *:p<0.05, **:p<0.001 or ***:p<0.001. Red dashed line signifies the change of viability in corresponding controls.

At the day 10 of the experiment, viability change was affected significantly from the induction (p=0.006), frequency of applied mechanical stimulation (p<0.001) and the interaction between applied frequency and induction (p<0.001) according to the GLM output (Table 2. 1). For averaged results of exposure time and applied frequency, cells that received adipogenic induction showed 5% (p=0.006) lower viability compared to cells that were cultured only in growth media (Figure 2.6 a). For averaged results of exposure time and induction, significantly higher cell viability was observed in 75 Hz group compared to 30 Hz (15%, p=0.047), 45Hz (28%, p<0.001), 90Hz (19%, p=0.007) and 105Hz (26%, p<0.001) but between no other groups (Figure 2. 6b). For averaged results of only exposure time, in growth conditions, there was no significant difference in cell viability between different frequency groups (Figure 2. 6c). However, for the cells that received adipogenic induction, cells that received 75Hz signals showed significantly higher cell viability compared to all other applied frequencies (for 30 Hz; 30% and p=0.002, for 45Hz; 64% and p<0.001, for 60Hz; 40% and p<0.001, for 90Hz; 28% and p=0.003, for 105 Hz; 48% and p<0.001, for 120 Hz; 27% and p=0.022) (Figure 2. 6d). Finally, the differences between cell viability between growth and adipogenic conditions between different applied frequencies was only significant at 45 Hz (28% difference, p=0.024).

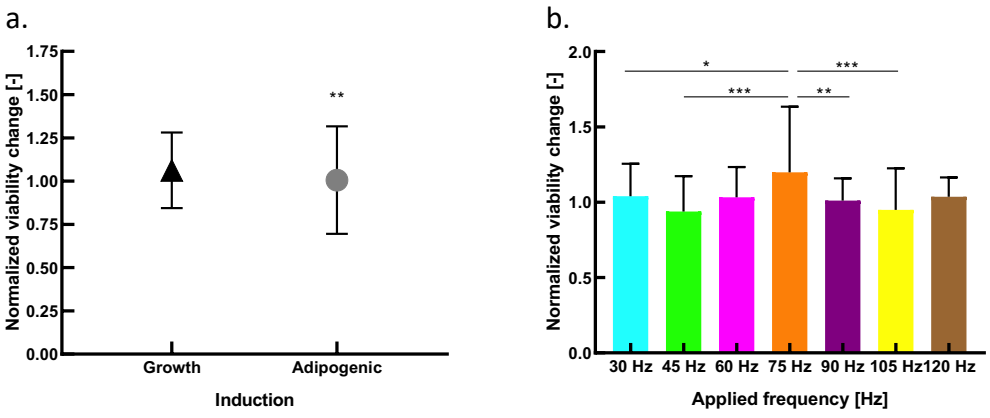

(cont.)

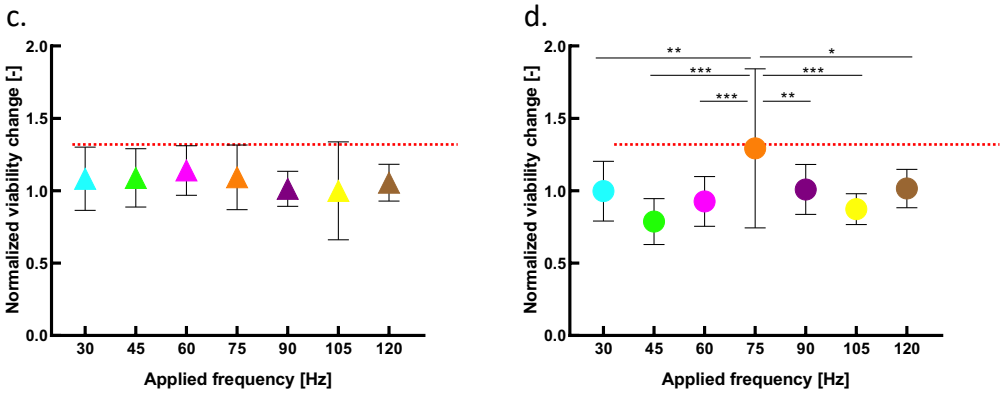

Figure 2. 6. Viability change of 3T3-L1 cells from day 1 to day 10 that is normalize to controls grouped based on **(a)** only induction media they received or **(b)** only applied frequency they received. Furthermore results were also represented for cells that **(c)** received growth induction grouped for applied frequency and **(d)** received growth induction grouped for applied frequency. Significant differences between groups were found by Tukey post-hoc tests and depicted with *:$p<0.05$, **:$p<0.001$ or ***:$p<0.001$. Red dashed line signifies the change of viability in corresponding controls.

2.4 Discussion

In this study, we have assessed the changes in the viability of preadipocytic 3T3-L1 cells that were exposed to LIV signals of different frequency and durations. Our study design involved 7 different frequency (30, 45, 60, 75, 90, 105 and 120 Hz); 3 different daily exposure duration (5, 10 and 20 min/day), 5 different experimental time points (1, 3, 5, 8 and 10 days) and 2 different culture conditions (quiescent and adipogenic), amounting to a total of 210 variations. Results showed in general adipogenic induction as well as applied LIV frequency had significant effects on cell viability, while exposure duration had not. Furthermore, applied to quiescent cells LIV signals did not change cell viability but adipogenic cells showed frequency specific increases in response to LIVs.

Based on the number of experimental groups we had to limit the outcomes of this study to viability results only, based on simple and low-cost testing availability [145]. However, our approach can be utilized in many different experimental designs where LIV signals were previously used with arbitrary parameters. In future studies, we are planning to explore the effects of novel frequencies we have identified here on the mechanisms of adipogenesis, such as lipid accumulation [146, 147], biochemical products [148], mRNA

expression [149, 150] and single-cell density [82]. Another limitation of our study was that we varied the duration and frequency of the LIV signal, but not the magnitude. Since the magnitude of mechanical loads are known to be biologically relevant [33, 151, 152], future studies should also involve variations in the LIV magnitude.

Testing the effect of mechanical signal components for different biological outcomes has been studied before with different goals previously. For example, LIV signals were applied during the osteogenesis of periodontal ligament stem cells at 0.3g magnitude and 30 min/day duration, with different frequencies ranging from 10 to 180 Hz [112]. This study showed a frequency dependent response related to osteogenic markers such as ALPase activity and Collagen Type 1, osterix, OCN and Runx2 mRNA expression levels. Markers that suggest to enhanced osteogenesis were observed at 40-50 Hz applied frequency range. However, in contrast to our results, the authors reported a stimulus related suppression of proliferation. Increased proliferation during osteogenesis is a repeatedly observed phenomenon for LIV exposed mesenchymal cells of bone marrow [83, 153] or adipose tissue [154]. Varied frequency (30, 400 and 800 Hz) LIV application (0.3g) further showed increased cell proliferation of human BMSCs for most frequency values [88]. This discrepancy in inducing or suppressing the proliferation may be related to the observed differences in stem cell proliferation rate of bone marrow and dental origin, where dental cells showed a consistently increased proliferation [155]. In a similar study where LIV signals were applied to human adipose tissue-derived MSCs (21 days for 10 min/day with 0.3g and 25, 35 and 45Hz frequencies), authors reported reduced expression of adipogenic differentiation genes and cell proliferation activity with increased frequencies, however the range of frequencies tested was not enough to be comparable with our study [94]. Furthermore, LIV signals (termed as sub-sonic vibrations) applied at 10, 20, 30 and 40 Hz frequencies on adipose tissue-derived MSCs for 4 days led to reduced proliferation and induced neurogenesis with suppressed adipogenesis, especially at 30 Hz applied frequency [97]. Another study showed that the application of LIV at 20 and 30 Hz frequencies suppressed the proliferation of 3T3-L1 preadipocytes and increase adipogenesis [101]. This study was conducted for 3 days, reported results on cell proliferation appears to be in aggreement to our results that at 30 Hz and after 3 days of stimulation 3T3-L1 cells showed lower viability compared to controls.

The lack of studies that focus on describing the components of mechanical stimulation is understandable, as it is quite challanging to standardize mechanical signal generation and used cell types. In conclusion, our study focused on the effect of

frequency, exposure time, experimental duration and adipogenesis induction on 3T3-L1 preadipocytes. Our results suggested that during quiescent growth mechanical stimulation induced a minor benefit on cell viability with indifference to applied frequency or exposure time. On the other hand, during adipogenesis, applied frequency became an important modulator of cell viability, with 75Hz signals resulted in the most increase in cell viability. Our results in general also suggested that compared to exposure time, the applied frequency was a more important determinant of cell viability.

CHAPTER 3

30, 45, 75 AND 90 Hz VIBRATIONS REDUCED THE GENE EXPRESSION, LIPID DROPLET PHYSIOLOGY AND CONCENTRATION ON 3T3-L1 CELLS DURING ADIPOGENESIS

3.1 Mechanical Signals and Adipogenesis

Bone marrow is a heterogeneous tissue that is composed of cells of hematopoietic and mesenchymal origin. Mesenchymal stem cells that reside in the bone marrow are capable of sustaining the bone formation and reformation however, it is also possible for them to differentiate into adipocytes, leading to bone marrow adipogenesis [156]. Current knowledge about bone marrow adipocytes is still limited but studies indicate that their origin, location, size and surface markers are different compared to white, brown or beige adipose tissue cells [157]. Adipocyte accrual in the bone marrow niche is known to be related to several physiological conditions such as aging, anorexia, obesity, osteoporosis and estrogen deficiency [158, 159], as well as external factors such as drug treatment and irradiation [160]. As bone marrow adipocytes are implicated as negative regulators of bone formation [161-163], prevention of adipogenesis can protect the skeletal health of individuals.

Individuals maintain bone tissue health by a process called remodelling throughout their life [164] and remodeling process is regulated by chemical signals such as oestrogens [165], parathyroid hormone [166], growth hormone [167], glucocorticoids [168] as well as physical signals [20, 22]. Thus, bone formation via mechanical loads is a favored strategy due to the fact that these loads are natural, omnipresent and nonpharmaceutical [132]. So that, planned physical activity must be integrated to the daily routine for a healthy bone structure, however, susceptibility to fractures of elderly people's bone make this integration difficult [29, 30]. Since bone is a dynamic organ, bone marrow adipogenesis can be repressed by mechanical forces such as gravity, blood pressure and muscle strains [10-19]. Hence, bone cells sense and respond to different forms of mechanical loads, including cyclic stretch [23], static pressure [24], shear stress [25, 26] and nanoscale mechanotransduction [27, 28].

Application of external mechanical signals in a low intensity vibration form (LIVs with magnitude lower than 1g gravitational force) is a preferable method to integrate

mechanical signals to daily routine with low risk and high compliance. Bone mineral density and bone area were shown to be significantly increased with the application of LIVs on postmenopausal and young women [16, 135, 169]. Moreover, the application of LIV significantly increased the osteoblast number, bone formation and bone mass after mechanical disuse [15]. Similarly, LIV signals increased the biomechanical properties of trabecular bone and its formation rate [14, 170]. Daily application of LIV signals in rodents are also effective in inhibiting adipogenesis in adipose and bone marrow tissue and reducing the triglyceride and nonesterified fatty acid content in liver [11, 15]. In vitro experiments also confirmed that application of LIV signals can increase osteogenesis and suppress adipogenesis. For example, daily application of LIVs with 0.3g, 25 Hz, 35 Hz and 45 Hz on human adipose tissue derived stem cells increased osteogenic differentiation capability of cells with increased osteocalcin and osteopontin mRNA expressions [93] while suppressing the adipogenic activity [94]. Similarly, application of LIVs with 0.1g, 90Hz on mouse mesenchymal stem cells increased the osteogenic differentiation with increased Runx2 mRNA expression [83] while decreasing the adipogenic differentiation with reduced expression levels of CEBPa and PPARg [144].

Even though related studies showed that daily application of LIV signals are suppressive for adipogenesis, most of these studies selected components of mechanical signals (e.g. exposure time, frequency and magnitude) as arbitrary parameters. The relationship between parameters of mechanical signal and and the biological response during adipogenesis is currently unknown. In this study, we aimed to understand the relationship between the applied frequency of LIV signals and biological response in mouse preadipocyte cells (3T3-L1) during adipogenic differentiation.

3.2 Materials and Methods

3.2.1 Cell Culture and Adipogenic Induction

3T3-L1 (ATCC CL-173) mouse embryo fibroblast cells were cultured in Dulbecco's Modified Eagle's Medium (Gibco, Ref#11320-074) with 10% new born calf serum (NBCS) (Biological Industries, Cat#716684) and 1% penicillin/streptomycin (Invitrogen, Cat#1092595) at 37 ºC, 5% CO2. Cells were passaged with 0.25% trypsin/EDTA solution (Biological Industries, Cat# 03-052-1B) at 37 °C, 5% CO2 for 5 min incubation before 1.2 rpm centrifugation for 5 min. 2 days after seeding of 3T3-L1

cells in plate, adipogenic induction was started by adding 5 µg/ml of insulin from bovine pancreas (Sigma, Lot#SLBD3067V), 10 nM of dexamethasone (Sigma, Lot#BCBK1265V) and 50 µM of indomethacine (Sigma, Lot#BCBF9122V) into growth medium. Cells were cultured at 37°C, 5% CO2 after starting the induction.

3.2.2 Application of Low Intensity Vibration (LIV) Signals

Mechanical signals were applied in vitro as previously described using vibrating platform as previously described [60, 83, 144]. Low intensity vibration (LIV) signals were applied at 0.1g but varied in frequency as 30Hz, 45Hz, 60Hz, 75Hz, 90Hz, 105Hz and 120Hz between subjects tuned using a software interface via MatLab for 10min/day. Cells received LIV signals up to 10 days under ambient conditions, while control groups received a sham treatment simultaneously.

3.2.3 Determination of Adipogenic Differentiation of 3T3-L1 Cells

3.2.3.1 Oil-Red-O Staining

Cells were washed with 0.5 ml of 1× PBS (×2) and fixed with 0.5 ml of 10% Neutral Buffered Formalin for 15 min at room temperature. Later, cells were rinsed with 0.5 ml of dH2O (×2) and stained with 0.5ml of 60% diluted 0.5% Oil-red-O in isopropanol (Amresco, Lot#1291C081) for 45 min at 37°C. Cells were rinsed with 0.5 ml of dH2O (×3). Stained samples were visualized by an inverted microscope (Olympus, IX-83).

3.2.3.2 Lipid Accumulation Measurements

3.2.3.2.1 Bodipy and DAPI Staining

At the end of 2-weeks control or treatment cells were stained with 0.5ml of 2µM BODIPY Staining solution (1:2500 in PBS) for 15 min at 37 °C at dark to visualize lipid accumulation. Then, cells were washed with phosphate buffered saline (PBS) three times and fixed with 4% paraformaldehyde (PFA) for 20min. PFA was triple washed with PBS followed by membrane permeabilization with 0.1% Triton X/PBS for 15 min. Cells were

blocked with 3% bovine serum albumin (BSA) in 0.1% Triton X/PBS for 30 min and were then incubated with 4',6-diamidino-2-phenylin-dole (DAPI) solution for visualization of nuclei. Images were acquired with an inverted microscope and fluorescent attachment at 20x magnification (Olympus, IX-83). 15 sample images were used per condition from at least two different experiments.

3.2.3.2.2 Image J Analysis

Each nuclei visualized via DAPI staining was counted for each image. Background was subtracted to eliminate noise. Image was zoomed and the lipid droplets in the each cell was labeled and counted. Number of cells analysed, how many of them did not have any droplet, number of droplets and the measurements of the droplets were transferred to excel. Total number of 270 images and 8543 cells were analyzed by using ImageJ software. Each lipid droplet in all cells were identified and their area, perimeter, mean and integrated density values were measured (Figure 3. 6).

3.2.3.2.3 Triglyceride Content Measurements

Intracellular triglyceride content was measured by the protocol of the Adipogenesis Colorimetric/Fluorometric Assay Kit (Biovision, Cat#K610-100). Lipid content of the 3T3-L1 cells was extracted by incubation at 90 oC for 30 min with 150µl of Lipid Extraction Solution provided by the kit itself. Extracted lipids were transferred to 96-well plate in the volume of 50µl. Then, 2 µl of lipase enzyme was added onto each well to convert triglyceride to glycerol and fatty acid. Later, 50 µl of reaction mix for each well was prepared by combining 46 µl of Adipogenesis Assay Buffer, 2 µl of Probe and 2 µl of Enzyme Mix which were provided by the kit, too. Mixtures were allowed to incubate at 37 oC for 30 min in the dark environment. OD measurements were taken at 570 nm at the end of 30 min incubation via VarioScan Spectrophotometer.

3.2.3.2.3.1 Triglyceride Content Calculations

Background was corrected by subtracting the value derived from 0 triglyceride standard from all readings. Standard curve was plotted. Sample readings were applied to

the standard curve. Triglyceride concentration was calculated by the division of triglyceride amount from standard curve into te sample volume.

3.2.3.3 Molecular expression of Adipogenic Genes

Cells were lysed and total mRNA was isolated using PureLink RNA mini kit (Invitrogen, USA). After verification of purity and determination of concentration with NanoDrop (ND-1000; Thermo Scientific, USA), two-step real-time PCR was performed. For reverse transcription reaction, RevertAid first strand cDNA synthesis kit (Thermo Scientific, USA) was used with 1000 ng template RNA. cDNA samples of 7.5 mL were loaded with 12mL of Sybr Green (Thermo Scientific, USA), 2.5mL forward and reverse primers of adipogenic markers, cEBPa and PPARg, for semiquantitative RT-PCR (Roche, USA), where GAPDH (glyceraldehyde 3-phosphate dehydrogenase) was used as the house-keeping molecule (Table 3. 1). For all groups, 3 samples were used for gene expression analysis.

Table 3. 2. Forward and reverse primer sequences of genes used for qRT-PCR expreiments.

cEBPa	F	TGG ACA AGA ACA GCA ACG AGT AC
	R	GCA GTT GCC CAT GGC CTT GAC
PPARg	F	GCC TTG CTG TGG GGA TGT C
	R	TCCTTGGCCCTCTGAGATGAG
GAPDH	F	GAC ATG CCG CCT GGA GAA AC
	R	AGC CCA GGA TGC CCT TTA GT

Table 3. 2. Protocol for qRT-PCR.

Preincubation	95ºC	600s	1 cycle
3 step amplification	95 ºC	30s	45 cycles
	60 ºC		
	72 ºC		
Melting	95 ºC	10s	1 cycle
	65 ºC	60s	
	72 ºC	1s	

3.2.4 Cell Density Measurements by Magnetic Levitation

The cells were resuspended to 105 cells/ml in the culture medium with Gd-based solution; gadobutrol (Gadavist®, Bayer) at a concentration of 25 mM $Gd3^{+}$,approximately 50 µl of cell suspension was loaded into the microcapillary channel (43). The cells were levitated in the magnetic levitation device and imaged after cells reached the equilibrium position (after about 10 min of levitation) under the inverted microscope (Olympus IX-83) (Fig 3. 2a,b.). Levitation heights of cells (distance of cells from the top surface of bottom magnet) were measured with ImageJ Fiji software by performing threshold and particle analysis [82].

3.2.5 Statistical Analyses

Results were presented as mean ± standard deviation. ANOVA followed by Tukey's post hoc test was used in order to detect significant differences between groups. Kruskal-Wallis test was used to contrast groups where results are distributed non-parametric. These results include magnetic levitation of adipocyte, where we use lower 0-5th% of the population based on single cell density, as well as triglyceride micrograph analysis results.

3.3 Results

3.3.1 Single Cell Density

3T3-L1 Cells that were either exposed to control or adipogenic conditions were measured for single cell density by magnetic levitation at Day 1, 3, 5, 8 and 10 of the culture (Fig. 3. 2a,b). For Day 1 and Day 3 mean single density of adipogenic cells were 0.08% and 0.18% smaller compared to control cells ($p<0.01$) However, after that adipogenic cells recorded higher mean single cell density values (0.61%, 0.55% and 0.33% , all $p<0.01$) compared to control cells. Based on the heterogenity of adipogenesis process and cell death observed in adipogenic cells, we decided to test only 5th% of the lowest single density cells (Fig.3. 2c.). When the all cells in quiescent group were analyzed in itself by comparing the effect of frequency on cell density, there was no significant group between control and vibrated groups (Fig. 3. 2d). When the 5th

percentile of the quiescent cells having the lowest density were analyzed, again there was no significant effect of any frequency on cell density (Fig.3. 2f). There was also no significant effect of any of the frequencies on the density of adipogenicly induced cells (Fig. 3. 2e.). However, when the 5th percentile of the adipogenicly induced cells having the lowest density was analyzed, 75 Hz showed significant increase by 0.6% ($p<0.0001$) (Fig 3. 2g).

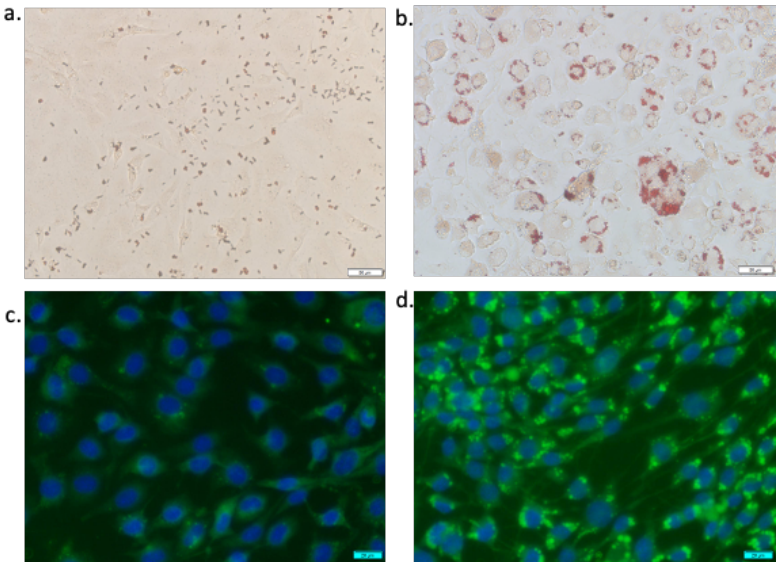

Figure 3. 1. Oil-red-o (top) and Bodipy (bottom) staining images of 3T3-L1 cells at day 10 under growt (left) and adipogenic (right) conditions.

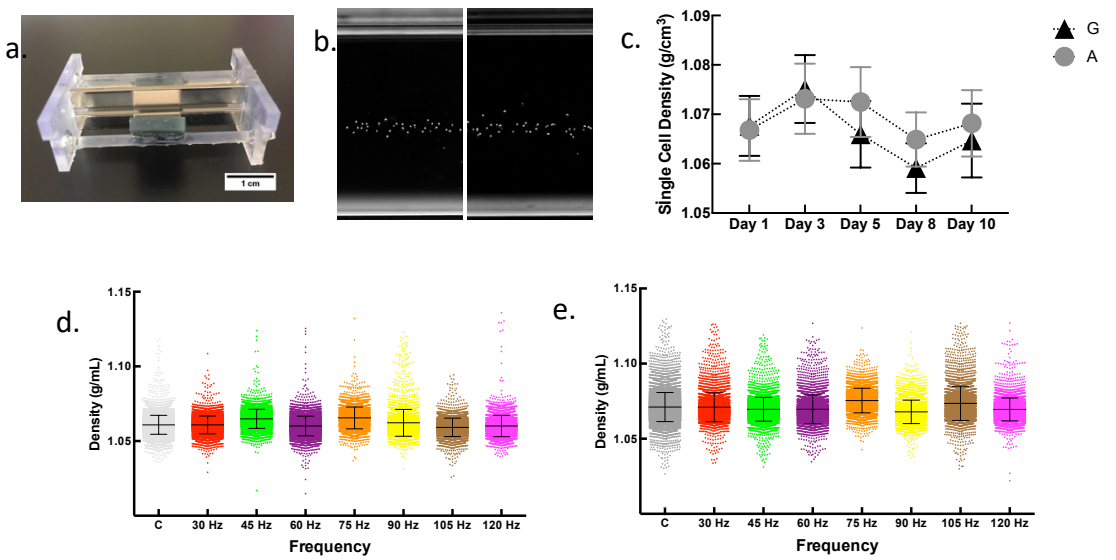

(cont.)

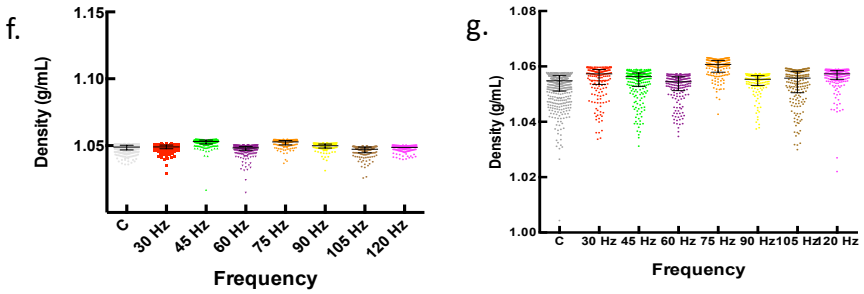

Figure 3. 2. Density of levitated adipogenic and quiescent cells **a.** levitation system. **b.** representing the levitated cells. **c.** Cell density of adipogenicly induced and quiescent cells at the end of 10 day-culture **d.** quiescent group and **e.** adipogenic group cell densities at day 10 after vibration. **f.** quiescent group and **g.** adipogenic group cell densities for 5% percentile subgroup.

3.3.2 Lipid droplets

Lipid accumulation of the cells were visualized by both oil-red-o staining (Fig. 3. 1a,c) and BODIPY staining (Fig. 3. 1b,d) Then, fluorescentşy stained lipid droplets were analyzed for quantification.

Adipogenic induction dramatically increased the lipid droplet areas by 9 fold ($p<0.0001$). All applied frequencies of low intensity vibrations significantly suppressed the average lipid droplet areas. 30 Hz, 45Hz, 60 Hz, 75 Hz, 90 Hz, 105 Hz and 120 Hz vibrations decreased the average lipid droplet areas by 55%, 75%, 19%, 34%, 10%, 29% and 41%, respectively (all $p<0.0001$) with the highest effect at 45 Hz. When the frequencies were compared, it was seen that the suppressive effect of frequency 60, 75, 90 and 105 was not significantly different from each other ($p>0.05$). Similarly, 75 Hz, 105 Hz and 120 Hz showed insignificant difference for lipid droplet area ($p>0.05$). (Fig. 3. 3a). When we look at the average perimeter value of all droplets in one cell (Fig 3. 3b), average perimeter of the lipid droplets accumulated in the cells was increased to 3.3 fold by adipogenic induction significantly ($p<0.0001$). 30 Hz, 45Hz, 60 Hz, 75 Hz, 90 Hz, 105 Hz and 120 Hz vibrations had significant decrease on average lipid droplet perimeter by 54%, 60%, 32%, 37%, 26%, 36% and 42% ($p<0.0001$) compared to AC group with a highest effect at 30 Hz. When the frequencies were compared, it was seen that the suppressive effect of frequency 30 Hz and 45 Hz was not significantly different from each other. Likewise, 60, 75, 90 and 105 Hz frequencies have a similar effect on lipid droplet perimeter with an insignificant difference between each other ($p>0.05$). Additionally, 75

Hz frequncy was not significantly different from 105 and 120 Hz as in the case of 105 Hz and 120 Hz comparison. Mean density signal coming from the lipid droplet per cell was significantly increased with the adipogenic induction by 9 fold significantly ($p<0.0001$). All frequencies, except 90 Hz, had significant decrease on mean density signal by 64% for 30 Hz, 92% for 45 Hz, 19% for 60 Hz, 34% for 75 Hz, 33% for 105 Hz and 40% for 120 Hz ($p<0.0001$). On the other hand, 60 Hz and 105 Hz, 75, 105 and 120 Hz, 105 and 120 Hz were not significantly different from each others (Fig. 3. 3c). Adipogenic induction significantly increased the integrated density per cell to 16 fold ($p<0.0001$). All frequencies had decreasing effect on integrated density except 90 Hz which had increased by 2% ($p<0.05$). 30Hz, 45 Hz, 60 Hz, 75 Hz, 105 Hz and 120 Hz frequencies decreased the integrated density by 75%, 78%, 43%, 57%, 59%, 68% respectively ($p<0.0001$). 60 Hz and 75 Hz, 75 Hz and 105 Hz, 105 Hz and 120 Hz were not significantly different from each others (Fig. 3. 3d).

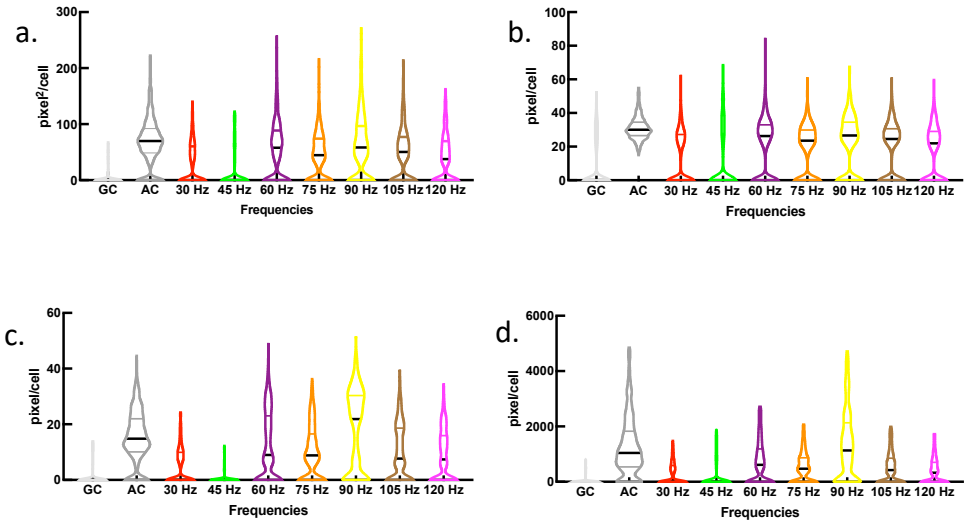

Figure 3. 3. Average area **(a)**, perimeter **(b)**, mean **(c)** and integrated density **(d)** values of lipid droplets after Image J analysis of bodipy stained images.

3.3.3 Triglyceride content

Triglyceride concentration in the adipogenic 3T3-L1 cells were 21% higher compared to growth control group, albeit this change was not statistically significant ($p>0.05$). However, 75 Hz LIV signals reduced the triglyceride concentration of the

adipogenic cells by 52% ($p<0.01$). On the other hand, triglyceride concentrations in 30 Hz and 120 Hz LIV groups were insignificantly different (7% and 27% lower, $p>0.05$) compared the adipogenic controls (Fig. 3. 4).

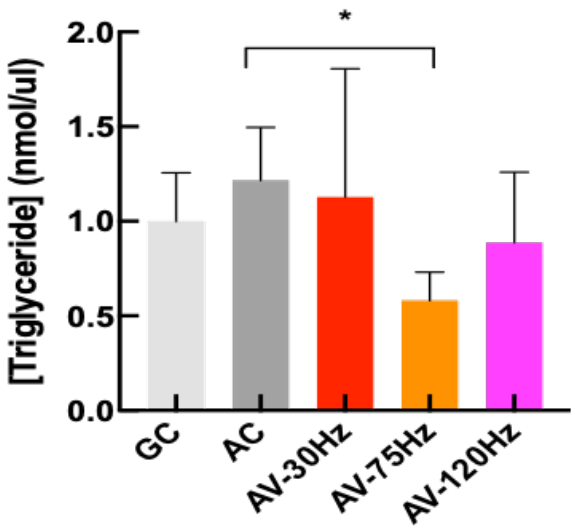

Figure 3. 4. Inner triglyceride concentration fold change pooled data at day 10 after vibration at defined frequencies.

3.3.4 Adipogenic mRNA markers

Adipogenic induction for 10 days increased the expression of cEBPa and PPARg significantly to 23 and 11 fold respectively ($p<0.05$ and $p<0.0001$) (Fig. 3. 5). 60 and 90 Hz vibrations reduced the normalized cEBPa expression by 79% and 81% decrease respectively ($p<0.005$). On the other hand, 30, 45, 75, 105 and 120 Hz frequencies decreased the expression of cEBPa insignificantly by 57%, 50%, 71%, 73% and 52%, respectively ($p>0.05$) (Fig. 3. 5a). In terms of the normalized expression of PPARg, all the frequency values were significantly effective on reduction in PPARg expression, where 30 Hz decreased by 61% ($p<0.05$), 45 Hz decreased by 76% ($p<0.01$), 60 Hz decreased by 80% ($p<0.01$), 75Hz showed the highest decrease by 94% ($p<0.001$), 90 Hz and 105 Hz decreased by 84% ($p<0.01$), and lastly 120 Hz decreased by 65% ($p<0.05$) (Fig. 3. 5b).

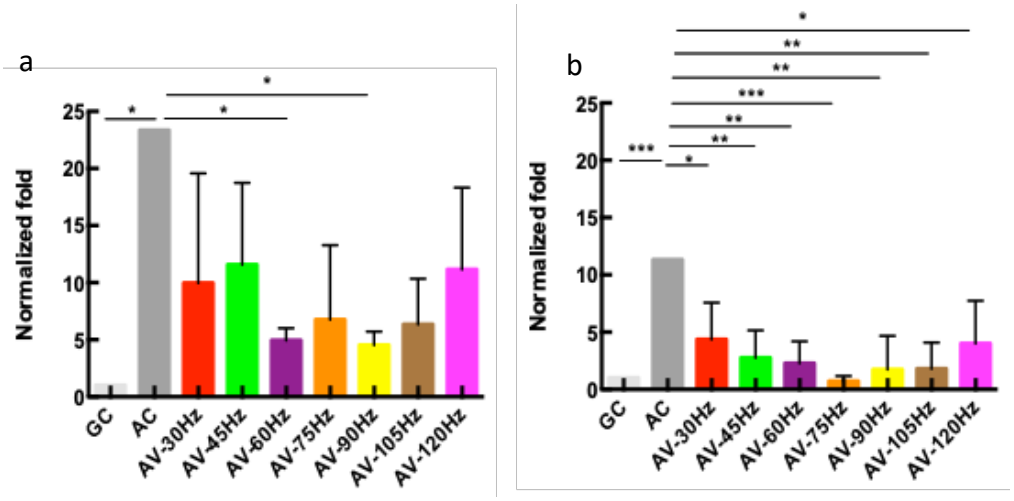

Figure 3. 5. Real-Time PCR **a.** CEBPa and **b.** PPARg gene expression normalized values at day 10 after vibration application at defined frequencies.

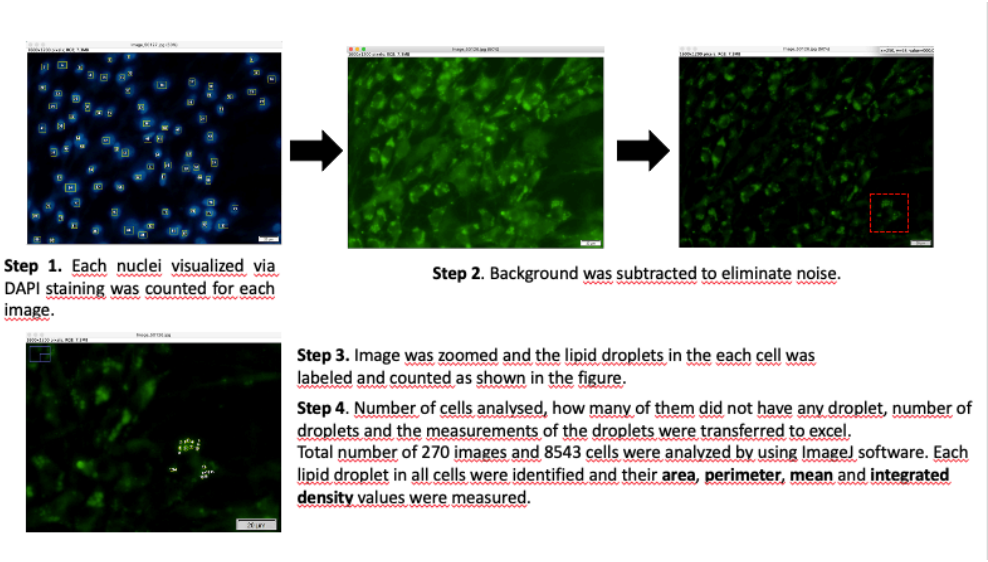

Figure 3. 6. Image J analysis steps of bodipy-stained-images.

3.4 Discussion

In this study, 7 different frequency values were tested to determine the most effective one during adipogenesis of 3T3-L1 preadiopcyte cells in terms of lipid droplet's physical qualifications, triglyceride content, cellular density and adipogenic gene expression level individually.

45 Hz vibration was the most effective frequency value for the reduction in lipid droplet area, mean density and integrated density of lipid droplets. In the literature, experiments performed with 45 Hz frequency showed that it was the optimal condition for whole body vibration [171], 45 Hz vibration with 3g applied on ovariectomized rats induced a further increase in periosteal bone formation rate and inhibited the endocortical resorption [172]. Furthermore, 45 Hz (0.3g) vibration was able to recover the decrease in trabecular bone mineral density of tail-suspended rats [173]. On the other hand, same regimen (45 Hz and 0.3g) was not effective in bone formation in trabecular or cortical bone in mice model [174].

Our study showed that 30 Hz vibration decreased the lipid droplet perimeter effectively which was increased due to adipogenic induction. Due to the fact that there is no study in the literature related to adipogenic differentiation and 30 Hz vibration relationship, it is said that 30 Hz vibration increased the skin blood flow on human subjects [175]. On the other hand, 30 Hz and 3g vibration was shown to increase cortical and medullary bone areas, likewise and of the periosteal and endosteal perimeters of ovariectomized rats [176]. On the other side, 30 Hz and/or 90 Hz 0.3g whole-body vibrations for 12 months did not induce any significant change in bone mineral density and bone structure in post- menopausal women [177]. 30 Hz whole-body vibration did not change the serum testosterone and insulin growth factor-1 levels of active adult males [178]. In molecular level, Runx-2 gene expression increased by the application of 30 Hz and 0.15g, 1g, 2g vibrations on mesenchymal stem cells [179].

Although 75 Hz was not preferred for the bone studies or any other vibrational studies, our study demonstrated that it was the most effective frequency value for reducing the triglyceride concentration in the cells showing the anti-adipogenic effect as well as decrease in the normalized expression level of PPARg. Normalized cEBPa gene expression was mostly reduced by the 90 Hz vibration which was effectibe on the D1-ORL mesenchymal stem cell differentiation previously [144].

In the study, density of the 3T3-L1 fibroblasts was determined as 1.06 ± 0.006 g/mL, slightly similar to literature reporting that the fibroblast had density of 1.05 g/mL [180]. This difference may result from origin of the cells. To our knowledge, the effect of vibration on single cell density has not been investigated before. Magnetic levitation analysis indicated that single cell density did not show a specific trend depending on increasing vibration frequency for both fibroblasts (uninduced cells) and adipogenic-induced cells. However, the changes in density mostly resulted in increasing at different

vibration frequencies, may cause from the impact of vibration on apoptosis [181] or transcriptional changes [182]. Interestingly, only at 75 Hz vibration in adipogenic group, it was observed a significant increase in the density, however, the reason of the situation is unclear. Besides, a decrease in the number of the cells whose density decreased due to lipid accumulation [82] was observed in adipogenic group with vibration. This may have occurred due to damage to adipocytes, which are known to be fragile, during vibration [82]. On the other hand, although we know that density changes in some physiological events [82, 183-185], there are still little information about when and how it is set and more research is needed.

CHAPTER 4

OSTEOGENIC DIFFERENTIATION OF MESENCHYMAL STEM CELLS ON RANDOM AND ALIGNED PAN/PPy NANOFIBROUS SCAFFOLDS

4.1. Tissue Engineering and Nanofibrous Scaffolds

Tissue engineering is a fast-growing field, which utilizes a combination of scaffolds, cells, and biologically active molecules to improve or restore anatomical and physiological functions [72]. Biological tissues are characterized by their mechanical, chemical and morphological properties that are mainly governed by extracellular matrix (ECM) proteins of that tissue. The main goal of tissue engineered scaffolds is to mimic the ECM for cells that are aimed to be grown, and most scaffolds are fabricated from polymers via various methods such as solvent casting and particulate leaching, melt molding, rapid prototyping, phase separation, and electrospinning [72]. Among these methods, electrospinning provides nanofibers with excellent interconnectivity [72], and porosity for the integration of cells into the scaffold with an appropriate pore size [116]. Therefore, electrospun polymer nanofibers became a frequently used tool in tissue engineering [186] and drug delivery [187-190] applications.

Electrospun nanofibrous scaffolds can be engineered to closely mimic the ECM based on their tunable mechanical, chemical, degradative and surface properties [74]. Various scaffold types for biomedical applications spanning from nerve to bone tissue engineering can be studied with electrospinning methodology based on the versatility in its nature [72]. An important aspect that governs the mechanical properties of various tissues including skeletal muscle, nerve, and vasculature is their anisotropic structure. These tissues show high elasticity in the direction of their extracellular matrix fibers alignment [44]. The fabrication methodology of electrospun nanofibers can easily be extended to align fibers during the collection process leading to the formation of aligned structures that promote the growth of cells neural, muscle and spinal disc applications [186, 191, 192].

Bone tissue is also known to be anisotropic [10]. It is therefore not surprising that several studies investigated effects of aligned synthetic or natural polymer electrospun fibers in bone tissue engineering applications [193-195]. In essence, aligned fibers enable

bone cell growth and alignment in the fiber directions. However, to date none of these studies used a biocompatible conductive polymer. Also, it is currently not known whether aligned fibers also facilitate calcification in the direction of alignment for bone cells.

For this study, we used Polypyrrole (PPy), which is a conductive polymer with known biocompatibility [193-195]. PPy is non-toxic and thin films made of PPy support attachment, adhesion and the osteogenic differentiation of mesenchymal stem cells as well [74]. Here we, developed 3D polyacrylonitrile (PAN)/PPy scaffolds by an electrospinning method and tested for osteogenic differentiation of mesenchymal stem cells. It was found that these nanofibers supported attachment, proliferation, and differentiation of mesenchymal stem cells. In addition, nanofiber alignment governed the direction of mineralization during osteogenesis, showing that PAN/PPy conductive scaffold is a potential candidate for bone tissue applications.

4.2. Materials and Methods

4.2.1. Osteogenic Differentiation of Mesenchymal Stem Cells on PAN/PPy Nanofibrous Scaffold

In this study, D1 ORL UVA (ATCC) bone marrow stem cells were used as a biological model [196]. PAN/PPy nanofibers on coverslips were sterilized by incubation at 200 ^{o}C for 3 h and then cells were seeded on nanofibers in 24-well cell culture plates at 500 cell/well density. Cells were grown until day 7, 14 and 21 for morphological assessment by SEM and viability assessment by MTT assay. D1 ORL UVA mesenchymal stem cells were either grown quiescent (DMEM + 10% FBS + 2%Pen/Strep) or induced 50% and 100% osteogenic medium. First tried osteogenic media was quiescent media + 10nM β-glycerolphosphate and 50μg/ml ascorbic acid [72] and the second was quiescent media + dexamethasone.

4.2.2. Characterization of cells

After 7, 14 and 21 days of culture, morphology of cells were analyzed with SEM. Cells were washed with phosphate-buffered saline (PBS) and then fixed with 4% paraformaldehyde for 3-4 h at room temperature. After fixation, cells were washed with

PBS and ultrapure water and then air dried. Dry cellular constructs were sputter coated with gold and observed under the SEM at an accelerating voltage of 5 kV.

Cell viability was determined by MTT (3-(4,5-Dimethylthiazol-2-yl)-2,5-diphenyltetrazolium bromide) assay. Culture medium was replaced with 10% MTT solution containing medium and the plates were incubated at 37°C, 5% CO2 for 4 h. During the incubation, the active enzymes of the viable cells transformed the yellow MTT into purple formazan crystals. The top medium was then removed and DMSO was added to each well to dissolve the formazan crystals. The absorbance of the solution was measured at 570 nm and 650 nm (Thermo Multiskan).

Presence of calcified matrix on PAN/PPy electrospun nanofibers was detected with Alizarin Red and Von Kossa staining at 21 days of quiescent or osteogenic culture of D1 ORL UVA cells. Cells were first washed with 1 ml of PBS (x3) and then fixed with 500 µl of 10% neutral buffered formalin for 30 min. Afterwards, cells were washed again (x2) with 1 ml of deionized (DI) water and stained with 1 ml of alizarin red dye for 30 min. After staining, cells were rinsed (x2) with DI water, and washed in PBS for 15 min to remove non-specific binding of dye. Micrographs of calcified matrix were taken through the light field of an inverted microscope (Olympus, IX-83).

For von Kossa staining firstly cells were fixed with 4% pfa for 20 min. Subsequently, PBS was discarted on the cells fixed in tissue culture plate and rinsed with DI water. 1 ml of a 1% silver nitrate solution was added and the plate was placed under UV light in laminar flow for 30 min. After incubation, cells were rinsed in DI water several times. Then, to remove unreacted silver 500 µl of 5 % sodium thiosulfate was put and incubeted for 5 min. Lastly, cells were rinsed with DI water again and kept the water inside the wells until observation under light microscope.

4.2.3. Statistics

All results were reported as mean ± standard deviation. Statistical comparions were made by Student's t-test in excel.

4.3.Results and Discussion

SEM images illustrated randomly distributed D1 ORL UVA mesenchymal stem cells on two dimensional glass surface (Fig. 4. 1). D1 cells attached and spread on glass

in both growth medium (GM) and osteogenic medium (OM). Consistent with literature [83], D1 cells that were cultured in OM for 21 days showed mineralization. D1 cells were able to attach randomly oriented PAN/PPy nanofibers for both growth and osteogenic conditions as evidenced by SEM images (Fig. 4. 2). Cells formed intimate contact with multiple fibers and displayed rough topography. D1 cells, that normally form extremely packed colonies in the absence of an ECM [197], initially formed distinct colonies but after 3 weeks of culture, they covered the whole surface of nanofibers and mineralization was observed for cells that were grown in osteogenic conditions. D1 cells that were cultured on aligned PAN/PPy nanofibers, depicted a cellular morphology that aligned and elongated in accordance to the fiber alignment direction (Fig. 4. 3). This observation was valid for cells both grown in quiescent and osteogenic conditions.

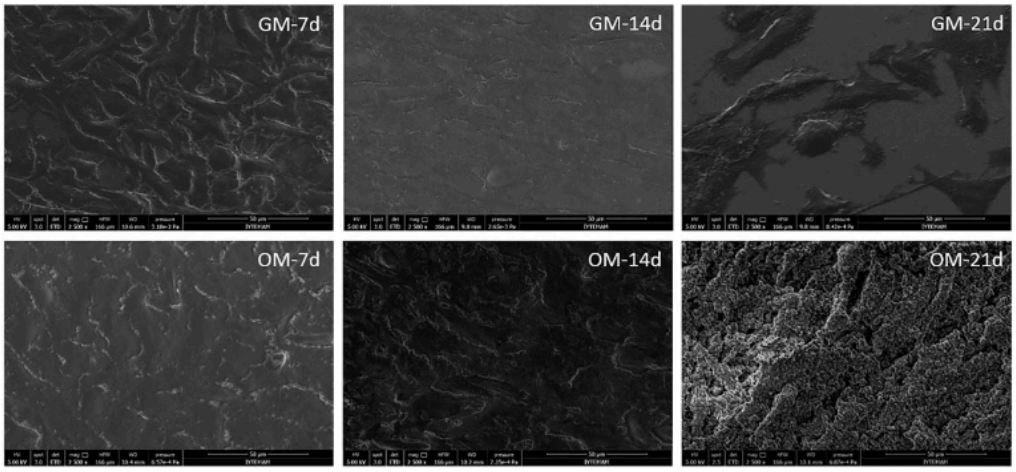

Figure 4. 1. SEM images of MSCs after culturing in growth medium (GM) and in osteogenic medium (OM) for 7, 14 and 21 days on glass control coverslips.

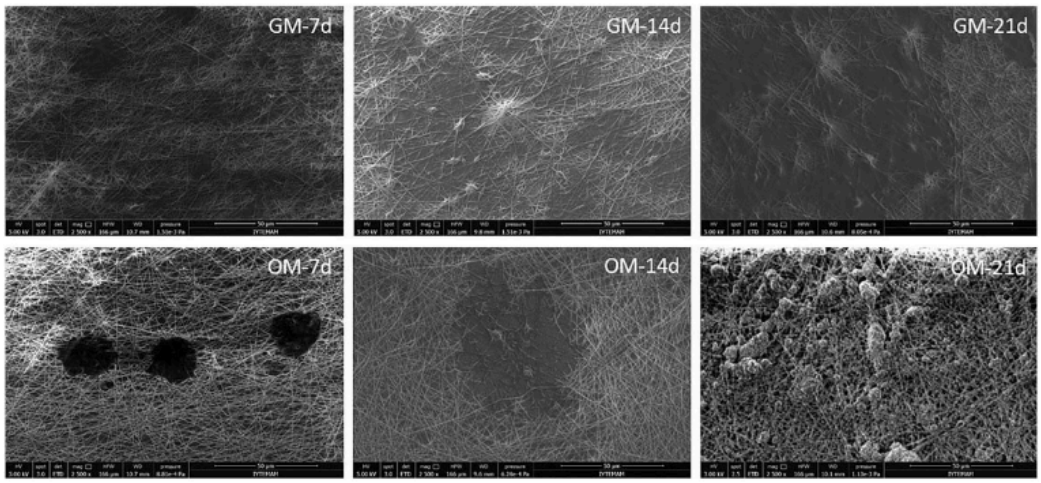

Figure 4. 2. SEM images of MSCs after culturing in growth medium and osteogenic medium for 7, 14 and 21 days on the random PAN/PPy nanofibers (250 rpm).

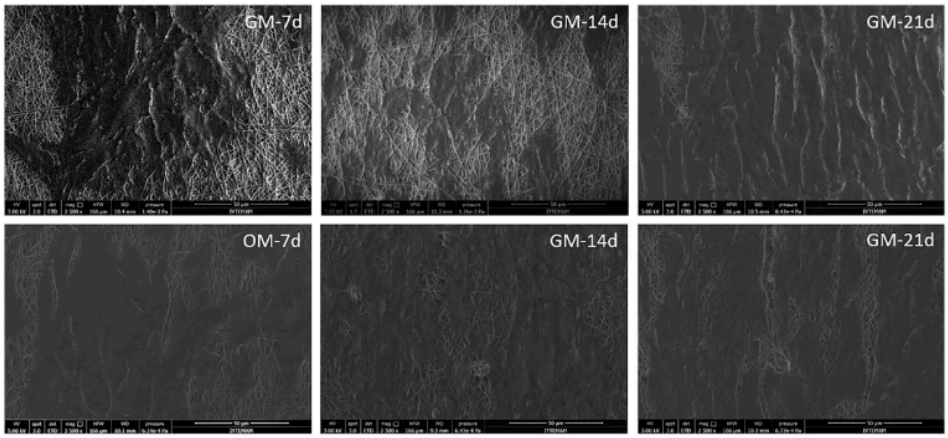

Figure 4. 3. SEM images of MSCs after culturing in growth medium and osteogenic medium for 7, 14 and 21 days on the aligned PAN/PPy nanofibers (1000 rpm).

In order to understand the degradation behavior of PAN/PPy nanofibers in culture conditions, both random and aligned nanofibers were put into the growth and osteogenic medium without inoculation of cells for 21 days. SEM images of nanofibers indicated that after 21 days, the morphology of fibers did not appear to change (Fig. 4. 4, Table 4. 1).

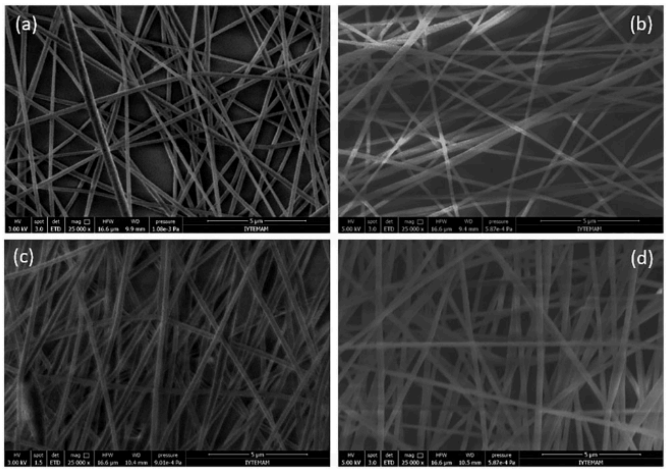

Figure 4. 4. SEM images of random nanofibers kept in (a) GM (b) OM , and aligned nanofibers kept in (c) GM, (d) OM after 21 days.

Table 4. 2. Average fiber diameter for random and aligned nanofibers after keeping in OM and GM for 21 days (without cell seeding).

	Random NFs	Aligned NFs
Ave. diameter	268 (±49)	225 (±72)
Ave. diameter (GM)	262 (±40)	248 (±53)
Ave. diameter (OM)	283 (±67)	235 (±39)

GM: growth medium; OM: osteogenic medium.

Proliferation of the D1 ORL UVA mesenchymal stem cells cultured on glass surface and PAN/PPy nanofibers were evaluated by MTT assay. Cells were able to proliferate on glass, randomly oriented and aligned PAN/PPy fibers similarly during 3 weeks of cell culture (Fig. 4. 5). Cell proliferation was similar for cells that were cultured in growth and osteogenic conditions, suggesting that PAN/PPy nanofibers were non-toxic for osteoblasts and could be utilized as scaffold for osteogenic differentiation of mesenchymal stem cells. These results are consistent with previous studies that showed D1 cells are as viable and active in 3D scaffolds as 2D surfaces [145]. The mineral deposition on PAN/PPy electrospun nanofibrous scaffolds was confirmed using Alizarin Red staining after the 21 days of incubation period. Results indicated that D1 ORL UVA mesenchymal stem cells cultured with both 50% dose (half-dose) and 100% dose (full-dose) osteogenic media was committed to osteogenesis, while cells in growth media did not show any mineral deposition (Fig. 4. 6). However, mineral deposition observed in full-dose osteogenic media was more distinct at the end of 3wks compared to half-dose. Furthermore, oriented mineral deposition was observed in scaffolds with aligned fibers, while mineralization was randomly oriented in 2D glass culture and non-oriented fiber scaffolds. While dexamethasone was induced for osteogenesis increased mineral deposition was noticed for half-dose osteogenic media compared to osteogenic media including β-glycerolphosphate and ascorbic acid, but there was not a significant advantage of dexamethasone in osteogenesis for full-dose. Alternative staining using von Kossa method showed similar calcification trends in control and experimental groups, consistent with Alizarin staining (Fig. 4. 7). Calcium staining was not observed in growth

medium in von Kossa staining however, in osteogenic group, von Kossa staining showed calcification.

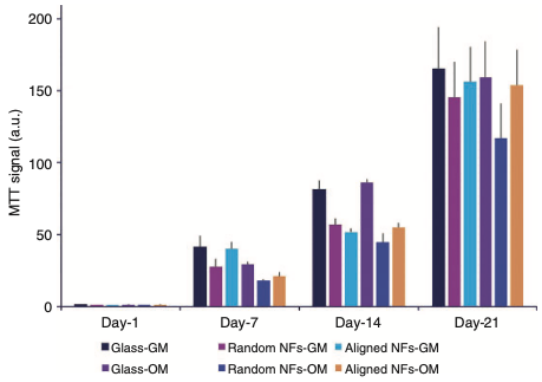

Figure 4. 5. MTT assay of D1 ORL UVA mesenchymal stem cells on 2D glass surface or in PPy nanofiber scaffolds after 1, 7, 14 and 21 days of culture. r: randomly oriented; a: aligned; GM: growth media; OM: Osteogenic media

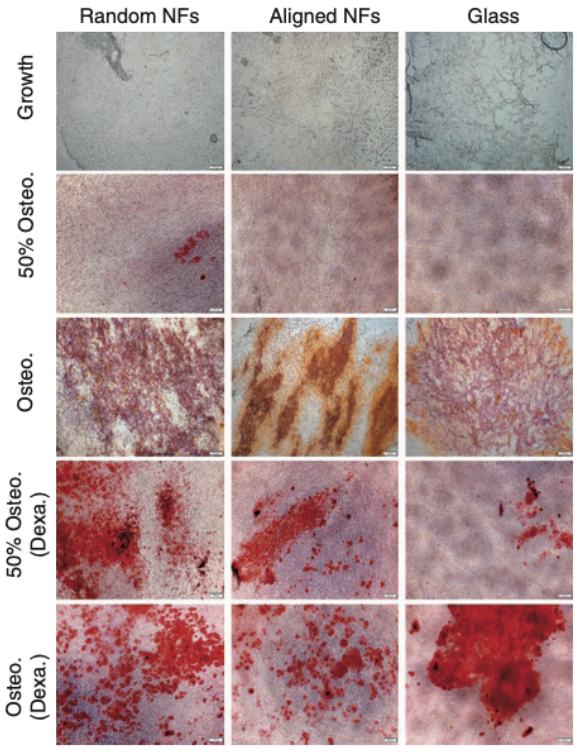

Figure 4. 6. Alizarin red staining on random NFs, aligned NFs and glass control for growth and (50% and 100%) osteogenic conditions after 21 days. Scale bar is 200 µm.

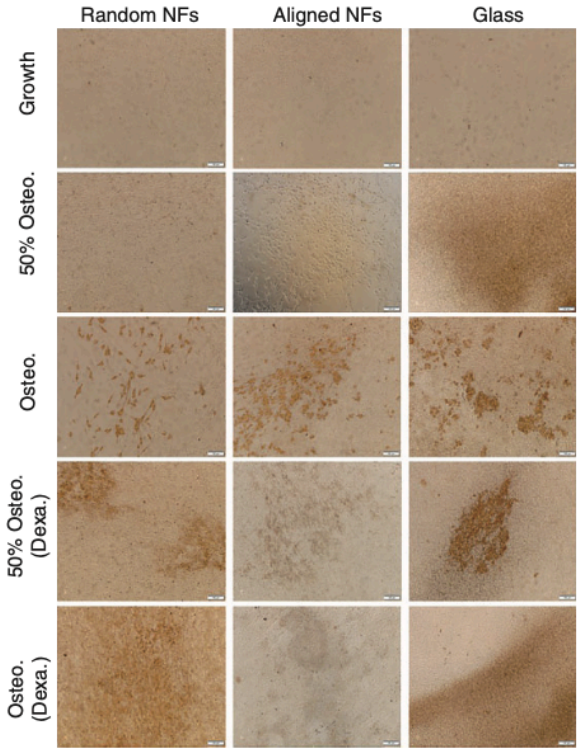

Figure 4. 7. Von Kossa staining after on random NFs, aligned NFs and glass control for growth and (50% and 100%) osteogenic conditions 21 days. Scale bar is 100 µm.

Chitosan electrospun nanofibrous scaffolds were also studied for osteoblast-like cells [198]. While the majority of observed osteoblast-like cells were in spindle morphology, the cells were expanded on nanofibrous scaffold relatively better compared to osteoblast-like cells grown on control chitosan film. PLLA/PCL/hydroxyapatite (HAP) electrospun nanofibers was another scaffold tested for the mouse calvaria-derived pre-osteoblastic cells (MC3T3-E1). This scaffold exhibited a good attachment and proliferation of osteoblasts and differentiation also was facilitated with this scaffold [199, 200]. PVA thin layer was deposited on electrospun nylon 6 hybrid nanofibers by a hydrothermal process were found to be very effective for bone tissue regeneration [201]. Gelatin electrospun fibrous scaffolds also supported adhesion and proliferation of osteoblasts and osteo-differentiation of mesenchymal stem cell [202]. Cross-linked boron-nitride reinforced gelatin electrospun scaffold was examined for human bone cells and showed nontoxic and biodegradable behavior [203]. It is confirmed that PAN/PPy is a suitable to use as a bone tissue engineering scaffold with its mineralization ability. Generally, many polymeric materials including natural and synthetic polymers in their fiber form have

been developed for bone tissue engineering [204]. However, the crucial thing is to find a scaffold supporting the adhesion, proliferation and differentiation of mesenchymal stem cells for bone tissue engineering. In this study, PAN/PPy nanofibers as a new material for osteogenic differentiation of mesenchymal stem cells with their random and aligned forms supported osteogenic differentiation of mesenchymal stem cells and indicated good viability for osteoblasts.

Scaffold mechanical properties and cell-cell interaction are two significant parameters that regulate osteogenic differentiation of mesenchymal stem cells [205]. Our results also suggested that mechanical properties of scaffold played a major role in cell viability. Cell viability on aligned nanofibers, which indicated higher strength, were higher than random nanofibers.

CHAPTER 5

CONCLUSION

This research thesis can be divided into three parts: the first part was designed to investigate the effect of seven different low intensity vibrational frequency values and the duration time of these frequencies on the viability of 3T3-L1 preadipocyte cell line under growth conditions and adipogenic induction. The second part was designed as a result of first part and since the duration time has no significant effect on viability, this time only the frequency effect was studied for the adipogenesis-related characters: lipid droplet accumulation quantifications, cellular density changes, adipogenic marker gene expressions and triglyceride concentration. The last part of the research focuses on the conductive polymer polypyrole as a candidate biomaterial inducing the osteogenic differentiation of mesenchymal stem cells. The entire study concerns about the low intensity vibrational forces and their actions on cell differentiation.

In Chapter 2, low intensity vibrations in tested frequencies was shown to be ineffective on viability of 3T3-L1 cells under growth conditions as well as the exposure duration. However, same frequency signals were able to modulate the cell viability during adipogenic differentiation especially 75 Hz signals resulted in the most increase in cell viability at day 10.

As mentioned in Chapter 3, 45 Hz signals was the most effective in reducing the area, mean and integrated density of the lipid droplets accumulated by adipogenesis. On the other hand, 30 Hz signal was significant for the reduction in the perimeter of the lipid droplets. 75 Hz, which was effective on increasing the viability in the previous chapter, had the most significant effect on decreasing the triglyceride concentration and also, the normalized expression level of PPARg.

As indicated in Chapter 4, random and aligned oriented synthesized PAN/PPy nanofibers were found to be biocompatible for mesechymal stem cell differentiation and osteoblast growth. Alignment of nanofibers directed the mineralization pattern of the differentiated cells and osteogenesis was induced by the usage of this polymer as a scaffold.

The entire study demonstrated the importance of the choice of the frequency level in terms of different aspects. This research showed that it is possible to change the

outcomes of the adipogenic differentiation, for example decrease the triglyceride concentration, expression level of adipogenic marker genes and/or lipid droplet area without changing the viability of the cells.

For a future projection, these results may contribute to the fine tuning of a mechanical stimulus regimen to combat adipogenesis. Regimens and devices tested so far in the literature that resulted in increased bone mineralization and density can be manipulated to provide not also increased bone structure but also decreased bone marrow adipogenesis. On the other hand, PAN/PPy nanofibers may find a suitable application in bone tissue engineering such as in the repair of bone defects, periosteum and reconstruction.

REFERENCES

1. Weiner, S.; Wagner, H. D., The material bone: structure-mechanical function relations. Annual Review of Materials Science 1998, 28 (1), 271-298.

2. Glimcher, M.; Muir, H., Recent studies of the mineral phase in bone and its possible linkage to the organic matrix by protein-bound phosphate bonds [and discussion]. Philosophical Transactions of the Royal Society of London B: Biological Sciences 1984, 304 (1121), 479-508.

3. Rho, J.-Y.; Kuhn-Spearing, L.; Zioupos, P., Mechanical properties and the hierarchical structure of bone. Medical engineering & physics 1998, 20 (2), 92-102.

4. Ruimerman, R., Modeling and remodeling in bone tissue. Technische Universiteit Eindhoven Eindhoven: 2005.

5. Bilezikian, J. P.; Raisz, L. G.; Martin, T. J., Principles of bone biology. Academic Press: 2008.

6. Rodan, G. A., The development and function of the skeleton and bone metastases. Cancer 2003, 97 (S3), 726-732.

7. Sommerfeldt, D.; Rubin, C., Biology of bone and how it orchestrates the form and function of the skeleton. European Spine Journal 2001, 10, S86-S95.

8. Väänänen, H. K.; Zhao, H.; Mulari, M.; Halleen, J. M., The cell biology of osteoclast function. J Cell Sci 2000, 113 (Pt 3), 377-381.

9. Salo, J.; Metsikko, K.; Palokangas, H.; Lehenkari, P.; Vaananen, H., Bone-resorbing osteoclasts reveal a dynamic division of basal plasma membrane into two different domains. Journal of Cell Science 1996, 109 (2), 301-307.

10. Arnsdorf, E. J.; Tummala, P.; Castillo, A. B.; Zhang, F.; Jacobs, C. R., The epigenetic mechanism of mechanically induced osteogenic differentiation. Journal of biomechanics 2010, 43 (15), 2881-2886.

11. Judex, S.; Lei, X.; Han, D.; Rubin, C., Low-magnitude mechanical signals that stimulate bone formation in the ovariectomized rat are dependent on the applied frequency but not on the strain magnitude. Journal of biomechanics 2007, 40 (6), 1333-1339.

12. Lau, E.; Al-Dujaili, S.; Guenther, A.; Liu, D.; Wang, L.; You, L., Effect of low-magnitude, high-frequency vibration on osteocytes in the regulation of osteoclasts. Bone 2010, 46 (6), 1508-1515.

13. Luu, Y. K.; Capilla, E.; Rosen, C. J.; Gilsanz, V.; Pessin, J. E.; Judex, S.; Rubin, C. T., Mechanical stimulation of mesenchymal stem cell proliferation and differentiation promotes osteogenesis while preventing dietary-induced obesity. Journal of Bone and Mineral Research 2009, 24 (1), 50-61.

14. Ozcivici, E.; Garman, R.; Judex, S., High-frequency oscillatory motions enhance the simulated mechanical properties of non-weight bearing trabecular bone. Journal of biomechanics 2007, 40 (15), 3404-3411.

15. Ozcivici, E.; Luu, Y. K.; Rubin, C. T.; Judex, S., Low-level vibrations retain bone marrow's osteogenic potential and augment recovery of trabecular bone during reambulation. PloS one 2010, 5 (6), e11178.

16. Rubin, C.; Recker, R.; Cullen, D.; Ryaby, J.; McCabe, J.; McLeod, K., Prevention of postmenopausal bone loss by a low-magnitude, high-frequency mechanical stimuli: a clinical trial assessing compliance, efficacy, and safety. Journal of Bone and Mineral Research 2004, 19 (3), 343-351.

17. Rubin, C.; Xu, G.; JUDEX, S., The anabolic activity of bone tissue, suppressed by disuse, is normalized by brief exposure to extremely low-magnitude mechanical stimuli. The FASEB Journal 2001, 15 (12), 2225-2229.

18. Sehmisch, S.; Galal, R.; Kolios, L.; Tezval, M.; Dullin, C.; Zimmer, S.; Stuermer, K.; Stuermer, E., Effects of low-magnitude, high-frequency mechanical stimulation in the rat osteopenia model. Osteoporosis international 2009, 20 (12), 1999-2008.

19. Verschueren, S. M.; Roelants, M.; Delecluse, C.; Swinnen, S.; Vanderschueren, D.; Boonen, S., Effect of 6-Month Whole Body Vibration Training on Hip Density, Muscle Strength, and Postural Control in Postmenopausal Women: A Randomized Controlled Pilot Study. Journal of bone and mineral research 2004, 19 (3), 352-359.

20. Heinonen, A.; Oja, P.; Kannus, P.; Sievanen, H.; Haapasalo, H.; Mänttäri, A.; Vuori, I., Bone mineral density in female athletes representing sports with different loading characteristics of the skeleton. Bone 1995, 17 (3), 197-203.

21. Lang, T.; LeBlanc, A.; Evans, H.; Lu, Y.; Genant, H.; Yu, A., Cortical and trabecular bone mineral loss from the spine and hip in long-duration spaceflight. Journal of bone and mineral research 2004, 19 (6), 1006-1012.

22. Meloni, M. A.; Galleri, G.; Pani, G.; Saba, A.; Pippia, P.; Cogoli-Greuter, M., Space flight affects motility and cytoskeletal structures in human monocyte cell line J-111. Cytoskeleton 2011, 68 (2), 125-137.

23. Gao, J.; Fu, S.; Zeng, Z.; Li, F.; Niu, Q.; Jing, D.; Feng, X., Cyclic stretch promotes osteogenesis-related gene expression in osteoblast-like cells through a cofilin-associated mechanism. Molecular medicine reports 2016, 14 (1), 218-224.

24. Zhang, L.; Liu, W.; Zhao, J.; Ma, X.; Shen, L.; Zhang, Y.; Jin, F.; Jin, Y., Mechanical stress regulates osteogenic differentiation and RANKL/OPG ratio in periodontal ligament stem cells by the Wnt/β-catenin pathway. Biochimica et Biophysica Acta (BBA)-General Subjects 2016, 1860 (10), 2211-2219.

25. Kim, K. M.; Choi, Y. J.; Hwang, J.-H.; Kim, A. R.; Cho, H. J.; Hwang, E. S.; Park, J. Y.; Lee, S.-H.; Hong, J.-H., Shear stress induced by an interstitial level of slow flow increases the osteogenic differentiation of mesenchymal stem cells through TAZ activation. PloS one 2014, 9 (3), e92427.

26. Zheng, L.; Chen, L.; Chen, Y.; Gui, J.; Li, Q.; Huang, Y.; Liu, M.; Jia, X.; Song, W.; Ji, J., The effects of fluid shear stress on proliferation and osteogenesis of human periodontal ligament cells. Journal of biomechanics 2016, 49 (4), 572-579.

27. Nikukar, H.; Reid, S.; Tsimbouri, P. M.; Riehle, M. O.; Curtis, A. S.; Dalby, M. J., Osteogenesis of mesenchymal stem cells by nanoscale mechanotransduction. ACS nano 2013, 7 (3), 2758-2767.

28. Pemberton, G. D.; Childs, P.; Reid, S.; Nikukar, H.; Tsimbouri, P. M.; Gadegaard, N.; Curtis, A. S.; Dalby, M. J., Nanoscale stimulation of osteoblastogenesis from mesenchymal stem cells: Nanotopography and nanokicking. Nanomedicine 2015, 10 (4), 547-560.

29. Kelley, G. A.; Kelley, K. S., Dropouts and compliance in exercise interventions targeting bone mineral density in adults: a meta-analysis of randomized controlled trials. Journal of osteoporosis 2013, 2013.

30. Mayoux-Benhamou, M.; Roux, C.; Perraud, A.; Fermanian, J.; Rahali-Kachlouf, H.; Revel, M., Predictors of compliance with a home-based exercise program added to usual medical care in preventing postmenopausal osteoporosis: an 18-month prospective study. Osteoporosis international 2005, 16 (3), 325-331.

31. Frost, H. M., Bone's mechanostat: a 2003 update. The Anatomical Record Part A: Discoveries in Molecular, Cellular, and Evolutionary Biology 2003, 275 (2), 1081-1101.

32. Robling, A.; Duijvelaar, K.; Geevers, J.; Ohashi, N.; Turner, C., Modulation of appositional and longitudinal bone growth in the rat ulna by applied static and dynamic force. Bone 2001, 29 (2), 105-113.

33. Fritton, S. P.; McLeod, K. J.; Rubin, C. T., Quantifying the strain history of bone: spatial uniformity and self-similarity of low-magnitude strains. Journal of biomechanics 2000, 33 (3), 317-325.

34. Gilsanz, V.; Wren, T. A.; Sanchez, M.; Dorey, F.; Judex, S.; Rubin, C., Low-level, high-frequency mechanical signals enhance musculoskeletal development of young women with low BMD. Journal of Bone and Mineral Research 2006, 21 (9), 1464-1474.

35. Reyes, M. L.; Hernández, M.; Holmgren, L. J.; Sanhueza, E.; Escobar, R. G., High-frequency, low-intensity vibrations increase bone mass and muscle strength in upper limbs, improving autonomy in disabled children. Journal of Bone and Mineral Research 2011, 26 (8), 1759-1766.

36. Ward, K.; Alsop, C.; Caulton, J.; Rubin, C.; Adams, J.; Mughal, Z., Low magnitude mechanical loading is osteogenic in children with disabling conditions. Journal of Bone and Mineral Research 2004, 19 (3), 360-369.

37. Matute-Llorente, A.; González-Agüero, A.; Gómez-Cabello, A.; Tous-Fajardo, J.; Vicente-Rodríguez, G.; Casajús, J., Effect of whole-body vibration training on bone mass in adolescents with and without Down syndrome: a randomized controlled trial. Osteoporosis International 2016, 27 (1), 181-191.

38. Lam, T.; Ng, B.; Cheung, L.; Lee, K.; Qin, L.; Cheng, J., Effect of whole body vibration (WBV) therapy on bone density and bone quality in osteopenic girls with adolescent idiopathic scoliosis: a randomized, controlled trial. Osteoporosis international 2013, 24 (5), 1623-1636.

39. Kiel, D. P.; Hannan, M. T.; Barton, B. A.; Bouxsein, M. L.; Sisson, E.; Lang, T.; Allaire, B.; Dewkett, D.; Carroll, D.; Magaziner, J., Low-Magnitude Mechanical Stimulation to Improve Bone Density in Persons of Advanced Age: A Randomized, Placebo-Controlled Trial. Journal of Bone and Mineral Research 2015, 30 (7), 1319-1328.

40. Lai, C.-L.; Tseng, S.-Y.; Chen, C.-N.; Liao, W.-C.; Wang, C.-H.; Lee, M.-C.; Hsu, P.-S., Effect of 6 months of whole body vibration on lumbar spine bone density in postmenopausal women: a randomized controlled trial. Clinical interventions in aging 2013, 8.

41. Slatkovska, L.; Alibhai, S. M.; Beyene, J.; Hu, H.; Demaras, A.; Cheung, A. M., Effect of 12 Months of Whole-Body Vibration Therapy on Bone Density and

Structure in Postmenopausal Women A Randomized Trial. Annals of internal medicine 2011, 155 (10), 668-679.

42. Wong, M.; Siegrist, M.; Cao, X., Cyclic compression of articular cartilage explants is associated with progressive consolidation and altered expression pattern of extracellular matrix proteins. Matrix biology : journal of the International Society for Matrix Biology 1999, 18 (4), 391-9.

43. Dordevic, S.; Tomazic, S.; Narici, M.; Pisot, R.; Meglic, A., In-vivo measurement of muscle tension: dynamic properties of the MC sensor during isometric muscle contraction. Sensors (Basel, Switzerland) 2014, 14 (9), 17848-63.

44. Barnes, G. R. G.; Pinder, D. N., In vivo tendon tension and bone strain measurement and correlation*. Journal of Biomechanics 1974, 7 (1), 35-42.

45. Manley, P. A.; Schatzker, J.; Sumner-Smith, G., Evaluation of tension and compression forces in the canine femur in vivo. Archives of orthopaedic and traumatic surgery 1982, 99 (3), 213-216.

46. Reneman, R. S.; Hoeks, A. P. G., Wall shear stress as measured in vivo: consequences for the design of the arterial system. Med Biol Eng Comput 2008, 46 (5), 499-507.

47. Yap, C. H.; Saikrishnan, N.; Tamilselvan, G.; Yoganathan, A. P., Experimental measurement of dynamic fluid shear stress on the aortic surface of the aortic valve leaflet. Biomech Model Mechanobiol 2012, 11 (1-2), 171-182.

48. Gooch, K. J.; Tennant, C. J., Mechanical Forces: Their Effects on Cells and Tissues. Springer: 1997.

49. Rubin, C. T.; Lanyon, L. E., Regulation of bone mass by mechanical strain magnitude. Calcif Tissue Int 1985, 37 (4), 411-7.

50. Srinivasan, S.; Weimer, D. A.; Agans, S. C.; Bain, S. D.; Gross, T. S., Low-magnitude mechanical loading becomes osteogenic when rest is inserted between each load cycle. Journal of bone and mineral research : the official journal of the American Society for Bone and Mineral Research 2002, 17 (9), 1613-1620.

51. Hsieh, Y. F.; Turner, C. H., Effects of loading frequency on mechanically induced bone formation. J Bone Miner Res 2001, 16 (5), 918-24.

52. Beck, B. R.; Kent, K.; Holloway, L.; Marcus, R., Novel, high-frequency, low-strain mechanical loading for premenopausal women with low bone mass: early findings. Journal of bone and mineral metabolism 2006, 24 (6), 505-7.

53. Ozcivici, E.; Kim Luu, Y.; Adler, B.; Qin, Y.-X.; Rubin, J.; Judex, S.; Rubin, C., Mechanical signals as anabolic agent in bone. 2010; Vol. 6, p 50-9.

54. Luu, Y. K.; Ozcivici, E.; Capilla, E.; Adler, B.; Chan, E.; Shroyer, K.; Rubin, J.; Judex, S.; Pessin, J. E.; Rubin, C. T., Development of diet-induced fatty liver disease in the aging mouse is suppressed by brief daily exposure to low-magnitude mechanical signals. International Journal Of Obesity 2009, 34, 401.

55. Judex, S.; Koh, T. J.; Xie, L., Modulation of bone's sensitivity to low-intensity vibrations by acceleration magnitude, vibration duration, and number of bouts. Osteoporosis International 2015, 26 (4), 1417-1428.

56. Gröning, F.; Fagan, M.; O'higgins, P., Comparing the Distribution of Strains with the Distribution of Bone Tissue in a Human Mandible: A Finite Element Study. The Anatomical Record 2013, 296 (1), 9-18.

57. Li, Y.; Li, Y.; Zhang, Q.; Wang, L.; Guo, M.; Wu, X.; Guo, Y.; Chen, J.; Chen, W., Mechanical Properties of Chondrocytes Estimated from Different Models of Micropipette Aspiration. Biophysical Journal 2019, 116 (11), 2181-2194.

58. Jiang, Z.; Harrington, P.; Zhang, M.; Marjani, S. L.; Park, J.; Kuo, L.; Pribenszky, C.; Tian, X., Effects of High Hydrostatic Pressure on Expression Profiles of In Vitro Produced Vitrified Bovine Blastocysts. Scientific Reports 2016, 6, 21215.

59. Kimura, H.; Nishikawa, M.; Yanagawa, N.; Nakamura, H.; Miyamoto, S.; Hamon, M.; Hauser, P.; Zhao, L.; Jo, O. D.; Komeya, M.; Ogawa, T.; Yanagawa, N., Effect of fluid shear stress on in vitro cultured ureteric bud cells. Biomicrofluidics 2018, 12 (4), 044107.

60. Olcum, M.; Ozcivici, E., Daily application of low magnitude mechanical stimulus inhibits the growth of MDA-MB-231 breast cancer cells in vitro. Cancer Cell International 2014, 14 (1), 102.

61. Pagnotti, G. M.; Adler, B. J.; Green, D. E.; Chan, M. E.; Frechette, D. M.; Shroyer, K. R.; Beamer, W. G.; Rubin, J.; Rubin, C. T., Low magnitude mechanical signals mitigate osteopenia without compromising longevity in an aged murine model of spontaneous granulosa cell ovarian cancer. Bone 2012, 51 (3), 570-577.

62. Ozcivici, E.; Garman, R.; Judex, S., High-frequency oscillatory motions enhance the simulated mechanical properties of non-weight bearing trabecular bone. J Biomech 2007, 40 (15), 3404-11.

63. Shikata, T.; Shiraishi, T.; Tanaka, K.; Morishita, S.; Takeuchi, R., Effects of Acceleration Amplitude and Frequency of Mechanical Vibration on Osteoblast-Like Cells. 2007.

64. Olcum, M.; Baskan, O.; Karadas, O.; Ozcivici, E., Application of low intensity mechanical vibrations for bone tissue maintenance and regeneration. Turkish Journal of Biology 2016, 40 (2), 300-307.

65. Kim, H.-J.; Kim, J.-H.; Song, Y.-J.; Seo, Y.-K.; Park, J.-K.; Kim, C.-W., Overexpressed Calponin3 by Subsonic Vibration Induces Neural Differentiation of hUC-MSCs by Regulating the Ionotropic Glutamate Receptor. Applied Biochemistry and Biotechnology 2015, 177 (1), 48-62.

66. El-Danasouri, I.; Sandi-Monroy, N. L.; Winkle, T.; Ott, K.; Krebs, C.; Maas, D. H. A.; Gagsteiger, F., Micro-vibration culture of human embryos improves pregnancy and implantation rates. Fertility and Sterility 2014, 102 (3), e217.

67. Hur, Y. S.; Park, J. H.; Ryu, E. K.; Park, S. J.; Lee, J. H.; Lee, S. H.; Yoon, J.; Yoon, S. H.; Hur, C. Y.; Lee, W. D.; Lim, J. H., Effect of micro-vibration culture system on embryo development. J Assist Reprod Genet 2013, 30 (6), 835-841.

68. Isachenko, E.; Maettner, R.; Isachenko, V.; Roth, S.; Kreienberg, R.; Sterzik, K., Mechanical agitation during the in vitro culture of human pre-implantation embryos drastically increases the pregnancy rate. Clinical laboratory 2010, 56 (11-12), 569-76.

69. Zhang, S.; Tan, Y.; Ren, Z.; Zhang, Y.; Zhang, S., A microchip laser feedback interferometer with nanometer resolution and increased measurement speed based on phase meter. Applied Physics B 2014, 116 (3), 609-616.

70. Reya, T.; Morrison, S. J.; Clarke, M. F.; Weissman, I. L., Stem cells, cancer, and cancer stem cells. Nature 2001, 414 (6859), 105-111.

71. Zakrzewski, W.; Dobrzyński, M.; Szymonowicz, M.; Rybak, Z., Stem cells: past, present, and future. Stem Cell Res Ther 2019, 10 (1), 68-68.

72. Abdal Dayem, A.; Lee, S. B.; Kim, K.; Lim, K. M.; Jeon, T.-I.; Seok, J.; Cho; Ssang, G., Production of Mesenchymal Stem Cells Through Stem Cell Reprogramming. Int J Mol Sci 2019, 20 (8), 1922.

73. Laronda, M. M.; Burdette, J. E.; Kim, J. J.; Woodruff, T. K., Recreating the female reproductive tract in vitro using iPSC technology in a linked microfluidics environment. Stem Cell Res Ther 2013, 4 (1), S13.

74. Anil-Inevi, M.; Yaman, S.; Yildiz, A. A.; Mese, G.; Yalcin-Ozuysal, O.; Tekin, H. C.; Ozcivici, E., Biofabrication of in situ Self Assembled 3D Cell Cultures in a Weightlessness Environment Generated using Magnetic Levitation. Sci Rep 2018, 8 (1), 7239.

75. Caplan, A. I., Adult mesenchymal stem cells for tissue engineering versus regenerative medicine. Journal of Cellular Physiology 2007, 213 (2), 341-347.

76. Dawson, E.; Mapili, G.; Erickson, K.; Taqvi, S.; Roy, K., Biomaterials for stem cell differentiation. Advanced drug delivery reviews 2008, 60 (2), 215-228.

77. Gurkan, U. A.; Akkus, O., The Mechanical Environment of Bone Marrow: A Review. Annals of Biomedical Engineering 2008, 36 (12), 1978-1991.

78. Gardner, O. F.; Alini, M.; Stoddart, M. J., Mesenchymal Stem Cells Derived from Human Bone Marrow. Methods in molecular biology (Clifton, N.J.) 2015, 1340, 41-52.

79. Ullah, I.; Subbarao, R. B.; Rho, G. J., Human mesenchymal stem cells - current trends and future prospective. Biosci Rep 2015, 35 (2), e00191.

80. Marion, N. W.; Mao, J. J., Mesenchymal stem cells and tissue engineering. Methods in enzymology 2006, 420, 339-61.

81. Baskan, O.; Mese, G.; Ozcivici, E., Low-intensity vibrations normalize adipogenesis-induced morphological and molecular changes of adult mesenchymal stem cells. Proceedings of the Institution of Mechanical Engineers, Part H: Journal of Engineering in Medicine 2017, 0954411916687338.

82. Sarigil, O.; Anil-Inevi, M.; Yilmaz, E.; Mese, G.; Tekin, H. C.; Ozcivici, E., Label-free density-based detection of adipocytes of bone marrow origin using magnetic levitation. Analyst 2019, 144 (9), 2942-2953.

83. Demiray, L.; Ozcivici, E., Bone marrow stem cells adapt to low-magnitude vibrations by altering their cytoskeleton during quiescence and osteogenesis. Turkish Journal of Biology 2015, 39 (1), 88-97.

84. Chen, B.; Lin, T.; Yang, X.; Li, Y.; Xie, D.; Zheng, W.; Cui, H.; Deng, W.; Tan, X., Low-magnitude, high-frequency vibration promotes the adhesion and the

osteogenic differentiation of bone marrow-derived mesenchymal stem cells cultured on a hydroxyapatite-coated surface: The direct role of Wnt/beta-catenin signaling pathway activation. International journal of molecular medicine 2016, 38 (5), 1531-1540.

85. Zhao, Q.; Lu, Y.; Yu, H.; Gan, X., Low magnitude high frequency vibration promotes adipogenic differentiation of bone marrow stem cells via P38 MAPK signal. PLOS ONE 2017, 12 (3), e0172954.

86. Lu, Y.; Zhao, Q.; Liu, Y.; Zhang, L.; Li, D.; Zhu, Z.; Gan, X.; Yu, H., Vibration loading promotes osteogenic differentiation of bone marrow-derived mesenchymal stem cells via p38 MAPK signaling pathway. Journal of biomechanics 2018, 71, 67-75.

87. Kim, I. S.; Song, Y. M.; Lee, B.; Hwang, S. J., Human Mesenchymal Stromal Cells are Mechanosensitive to Vibration Stimuli. Journal of Dental Research 2012, 91 (12), 1135-1140.

88. Chen, X.; He, F.; Zhong, D.-Y.; Luo, Z.-P., Acoustic-frequency vibratory stimulation regulates the balance between osteogenesis and adipogenesis of human bone marrow-derived mesenchymal stem cells. BioMed research international 2015, 2015, 540731-540731.

89. Prè, D.; Ceccarelli, G.; Visai, L.; Benedetti, L.; Imbriani, M.; Cusella De Angelis, M. G.; Magenes, G., High-Frequency Vibration Treatment of Human Bone Marrow Stromal Cells Increases Differentiation toward Bone Tissue. Bone marrow research 2013, 2013, 803450-803450.

90. Nikolaev, N. I.; Liu, Y.; Hussein, H.; Williams, D. J., The sensitivity of human mesenchymal stem cells to vibration and cold storage conditions representative of cold transportation. Journal of the Royal Society, Interface 2012, 9 (75), 2503-2515.

91. Bunnell, B. A.; Flaat, M.; Gagliardi, C.; Patel, B.; Ripoll, C., Adipose-derived stem cells: isolation, expansion and differentiation. Methods 2008, 45 (2), 115-120.

92. Frese, L.; Dijkman, P. E.; Hoerstrup, S. P., Adipose Tissue-Derived Stem Cells in Regenerative Medicine. Transfus Med Hemother 2016, 43 (4), 268-274.

93. Marędziak, M.; Lewandowski, D.; Tomaszewski, K. A.; Kubiak, K.; Marycz, K., The Effect of Low-Magnitude Low-Frequency Vibrations (LMLF) on Osteogenic Differentiation Potential of Human Adipose Derived Mesenchymal Stem Cells. Cellular and Molecular Bioengineering 2017, 10 (6), 549-562.

94. Marycz, K.; Lewandowski, D.; Tomaszewski, K. A.; Henry, B. M.; Golec, E. B.; Marędziak, M., Low-frequency, low-magnitude vibrations (LFLM) enhances

chondrogenic differentiation potential of human adipose derived mesenchymal stromal stem cells (hASCs). PeerJ 2016, 4, e1637.

95. Tirkkonen, L.; Halonen, H.; Hyttinen, J.; Kuokkanen, H.; Sievänen, H.; Koivisto, A.-M.; Mannerström, B.; Sándor George, K. B.; Suuronen, R.; Miettinen, S.; Haimi, S., The effects of vibration loading on adipose stem cell number, viability and differentiation towards bone-forming cells. Journal of The Royal Society Interface 2011, 8 (65), 1736-1747.

96. Pre, D.; Ceccarelli, G.; Gastaldi, G.; Asti, A.; Saino, E.; Visai, L.; Benazzo, F.; Cusella De Angelis, M. G.; Magenes, G., The differentiation of human adipose-derived stem cells (hASCs) into osteoblasts is promoted by low amplitude, high frequency vibration treatment. Bone 2011, 49 (2), 295-303.

97. Choi, Y. K.; Cho, H.; Seo, Y. K.; Yoon, H. H.; Park, J. K., Stimulation of sub-sonic vibration promotes the differentiation of adipose tissue-derived mesenchymal stem cells into neural cells. Life Sci 2012, 91 (9-10), 329-37.

98. Cho, H.; Seo, Y.-K.; Jeon, S.; Yoon, H.-H.; Choi, Y.-K.; Park, J.-K., Neural differentiation of umbilical cord mesenchymal stem cells by sub-sonic vibration. Life Sciences 2012, 90 (15), 591-599.

99. Edwards, J.; Reilly, G., Low magnitude, high frequency vibration modulates mesenchymal progenitor differentiation. Trans Annu Meet Orthop Res Soc 2011, 57.

100. Dulak, J.; Szade, K.; Szade, A.; Nowak, W.; Jozkowicz, A., Adult stem cells: hopes and hypes of regenerative medicine. Acta biochimica Polonica 2015, 62 (3), 329-37.

101. Oh, E.-S.; Seo, Y.-K.; Yoon, H.-H.; Cho, H.; Yoon, M.-Y.; Park, J.-K., Effects of sub-sonic vibration on the proliferation and maturation of 3T3-L1 cells. Life Sciences 2011, 88 (3), 169-177.

102. Gao, H.; Zhai, M.; Wang, P.; Zhang, X.; Cai, J.; Chen, X.; Shen, G.; Luo, E.; Jing, D., Lowlevel mechanical vibration enhances osteoblastogenesis via a canonical Wnt signalingassociated mechanism. Mol Med Rep 2017, 16 (1), 317-324.

103. Zhang, Y.; Hou, W.; Liu, Y.; Long, H.; Zhang, L.; Zhu, Z.; Yu, H., Microvibration stimulates β-catenin expression and promotes osteogenic differentiation in osteoblasts. Archives of Oral Biology 2016, 70, 47-54.

104. Ota, T.; Chiba, M.; Hayashi, H., Vibrational stimulation induces osteoblast differentiation and the upregulation of osteogenic gene expression in vitro. Cytotechnology 2016, 68 (6), 2287-2299.

105. Pongkitwitoon, S.; Weinheimer-Haus, E. M.; Koh, T. J.; Judex, S., Low-intensity vibrations accelerate proliferation and alter macrophage phenotype in vitro. Journal of Biomechanics 2016, 49 (5), 793-796.

106. Shafieyan, Y.; Tiedemann, K.; Komarova, S. V.; Quinn, T. M., Effects of low frequency cyclic mechanical stretching on osteoclastogenesis. Journal of Biomechanics 2014, 47 (15), 3750-3757.

107. Chen, F.-M.; Gao, L.-N.; Tian, B.-M.; Zhang, X.-Y.; Zhang, Y.-J.; Dong, G.-Y.; Lu, H.; Chu, Q.; Xu, J.; Yu, Y.; Wu, R.-X.; Yin, Y.; Shi, S.; Jin, Y., Treatment of periodontal intrabony defects using autologous periodontal ligament stem cells: a randomized clinical trial. Stem Cell Res Ther 2016, 7 (1), 33.

108. Seo, B.-M.; Miura, M.; Gronthos, S.; Mark Bartold, P.; Batouli, S.; Brahim, J.; Young, M.; Gehron Robey, P.; Wang, C. Y.; Shi, S., Investigation of multipotent postnatal stem cells from human periodontal ligament. The Lancet 2004, 364 (9429), 149-155.

109. Benjakul, S.; Leethanakul, C.; Jitpukdeebodintra, S., Effects of low magnitude high frequency mechanical vibration combined with compressive force on human periodontal ligament cells in vitro. European Journal of Orthodontics 2017, 40 (4), 356-363.

110. Zhang, C.; Lu, Y.; Zhang, L.; Liu, Y.; Zhou, Y.; Chen, Y.; Yu, H., Influence of different intensities of vibration on proliferation and differentiation of human periodontal ligament stem cells. Archives of medical science : AMS 2015, 11 (3), 638-646.

111. Shen, T.; Qiu, L.; Chang, H.; Yang, Y.; Jian, C.; Xiong, J.; Zhou, J.; Dong, S., Cyclic tension promotes osteogenic differentiation in human periodontal ligament stem cells. International journal of clinical and experimental pathology 2014, 7 (11), 7872-7880.

112. Zhang, C.; Li, J.; Zhang, L.; Zhou, Y.; Hou, W.; Quan, H.; Li, X.; Chen, Y.; Yu, H., Effects of mechanical vibration on proliferation and osteogenic differentiation of human periodontal ligament stem cells. Arch Oral Biol 2012, 57 (10), 1395-407.

113. Tang, N.; Zhao, Z.; Zhang, L.; Yu, Q.; Li, J.; Xu, Z.; Li, X., Up-regulated osteogenic transcription factors during early response of human periodontal ligament

stem cells to cyclic tensile strain. Archives of medical science : AMS 2012, 8 (3), 422-430.

114. Uzer, G.; Bas, G.; Sen, B.; Xie, Z.; Birks, S.; Olcum, M.; McGrath, C.; Styner, M.; Rubin, J., Sun-mediated mechanical LINC between nucleus and cytoskeleton regulates βcatenin nuclear access. Journal of Biomechanics 2018, 74, 32-40.

115. Tajik, A.; Zhang, Y.; Wei, F.; Sun, J.; Jia, Q.; Zhou, W.; Singh, R.; Khanna, N.; Belmont, A. S.; Wang, N., Transcription upregulation via force-induced direct stretching of chromatin. Nature materials 2016, 15 (12), 1287-1296.

116. Le, H. Q.; Ghatak, S.; Yeung, C. Y.; Tellkamp, F.; Gunschmann, C.; Dieterich, C.; Yeroslaviz, A.; Habermann, B.; Pombo, A.; Niessen, C. M.; Wickstrom, S. A., Mechanical regulation of transcription controls Polycomb-mediated gene silencing during lineage commitment. Nature cell biology 2016, 18 (8), 864-75.

117. Uzer, G.; Thompson, W. R.; Sen, B.; Xie, Z.; Yen, S. S.; Miller, S.; Bas, G.; Styner, M.; Rubin, C. T.; Judex, S.; Burridge, K.; Rubin, J., Cell Mechanosensitivity to Extremely Low-Magnitude Signals Is Enabled by a LINCed Nucleus. Stem cells (Dayton, Ohio) 2015, 33 (6), 2063-76.

118. Sen, B.; Xie, Z.; Case, N.; Styner, M.; Rubin, C. T.; Rubin, J., Mechanical signal influence on mesenchymal stem cell fate is enhanced by incorporation of refractory periods into the loading regimen. Journal of Biomechanics 2011, 44 (4), 593-599.

119. Hou, W. W.; Zhu, Z. L.; Zhou, Y.; Zhang, C. X.; Yu, H. Y., Involvement of Wnt activation in the micromechanical vibration-enhanced osteogenic response of osteoblasts. Journal of Orthopaedic Science 2011, 16 (5), 598-605.

120. Zhao, Q.; Lu, Y.; Gan, X.; Yu, H., Low magnitude high frequency vibration promotes adipogenic differentiation of bone marrow stem cells via P38 MAPK signal. PloS one 2017, 12 (3), e0172954.

121. Ingber, D., Mechanobiology and diseases of mechanotransduction. Annals of Medicine 2003, 35 (8), 564-577.

122. Ingber, D. E., Cellular mechanotransduction: putting all the pieces together again. The FASEB Journal 2006, 20 (7), 811-827.

123. Kim, D.-H.; Wong, P. K.; Park, J.; Levchenko, A.; Sun, Y., Microengineered Platforms for Cell Mechanobiology. Annual Review of Biomedical Engineering 2009, 11 (1), 203-233.

124. Mammoto, T.; Mammoto, A.; Ingber, D. E., Mechanobiology and Developmental Control. Annual Review of Cell and Developmental Biology 2013, 29 (1), 27-61.

125. Ozcivici, E.; Luu, Y. K.; Adler, B.; Qin, Y.-X.; Rubin, J.; Judex, S.; Rubin, C. T., Mechanical signals as anabolic agents in bone. Nature Reviews Rheumatology 2010, 6 (1), 50-59.

126. Wang, N.; Tytell, J. D.; Ingber, D. E., Mechanotransduction at a distance: mechanically coupling the extracellular matrix with the nucleus. Nature Reviews Molecular Cell Biology 2009, 10 (1), 75-82.

127. Wan-Young, C.; Purwar, A.; Sharma, A. In Frequency domain approach for activity classification using accelerometer, 2008 30th Annual International Conference of the IEEE Engineering in Medicine and Biology Society, 20-25 Aug. 2008; 2008; pp 1120-1123.

128. Booth, F. W.; Roberts, C. K.; Laye, M. J., Lack of exercise is a major cause of chronic diseases. Compr Physiol 2012, 2 (2), 1143-211.

129. Glatt, V.; Evans, C. H.; Stoddart, M. J., Regenerative rehabilitation: The role of mechanotransduction in orthopaedic regenerative medicine. Journal of Orthopaedic Research 2019, 37 (6), 1263-1269.

130. Ma, J.; Xia, M. D., Jing; Gao, J.; Lu, F.; Liao, Y., Mechanical Signals Induce Dedifferentiation of Mature Adipocytes and Increase the Retention Rate of Fat Grafts. Plastic and Reconstructive Surgery 2019, 144 (6), 1323-1333.

131. Monemian Esfahani, A.; Rosenbohm, J.; Reddy, K.; Jin, X.; Bouzid, T.; Riehl, B.; Kim, E.; Lim, J. Y.; Yang, R., Tissue Regeneration from Mechanical Stretching of Cell-Cell Adhesion. Tissue Eng Part C Methods 2019, 25 (11), 631-640.

132. Uzan, M. O.; Baskan, O.; Karadas, O.; Ozcivici, E., Application of low intensity mechanical vibrations for bone tissue maintenance and regeneration. Turkish Journal of Biology 2016, 40 (2), 300-307.

133. Choy, M.-H. V.; Wong, R. M.-Y.; Li, M.-C.; Wang, B. Y.; Liu, X. D.; Lee, W.; Cheng, J. C.-Y.; Chow, S. K.-H.; Cheung, W.-H., Can we enhance osteoporotic metaphyseal fracture healing through enhancing ultrastructural and functional changes of osteocytes in cortical bone with low-magnitude high-frequency vibration? The FASEB Journal 2020, 34 (3), 4234-4252.

134. Wong, R. M. Y.; Ho, W.-T.; Tang, N.; Tso, C. Y.; Ng, W. K. R.; Chow, S. K.-H.; Cheung, W.-H., A study protocol for a randomized controlled trial evaluating

vibration therapy as an intervention for postural training and fall prevention after distal radius fracture in elderly patients. Trials 2020, 21 (1), 95.

135. Chan, M. E.; Uzer, G.; Rubin, C. T., The Potential Benefits and Inherent Risks of Vibration as a Non-Drug Therapy for the Prevention and Treatment of Osteoporosis. Current Osteoporosis Reports 2013, 11 (1), 36-44.

136. DiVasta, A. D.; Feldman, H. A.; Rubin, C. T.; Gallagher, J. S.; Stokes, N.; Kiel, D. P.; Snyder, B. D.; Gordon, C. M., The ability of low-magnitude mechanical signals to normalize bone turnover in adolescents hospitalized for anorexia nervosa. Osteoporosis International 2017, 28 (4), 1255-1263.

137. Luu, Y. K.; Capilla, E.; Rosen, C. J.; Gilsanz, V.; Pessin, J. E.; Judex, S.; Rubin, C. T., Mechanical Stimulation of Mesenchymal Stem Cell Proliferation and Differentiation Promotes Osteogenesis While Preventing Dietary-Induced Obesity. Journal of Bone and Mineral Research 2009, 24 (1), 50-61.

138. Krishnamoorthy, D.; Frechette, D. M.; Adler, B. J.; Green, D. E.; Chan, M. E.; Rubin, C. T., Marrow adipogenesis and bone loss that parallels estrogen deficiency is slowed by low-intensity mechanical signals. Osteoporosis International 2016, 27 (2), 747-756.

139. Luu, Y.; Ozcivici, E.; Capilla, E.; Adler, B.; Chan, E.; Shroyer, K.; Rubin, J.; Judex, S.; Pessin, J.; Rubin, C., Development of diet-induced fatty liver disease in the aging mouse is suppressed by brief daily exposure to low-magnitude mechanical signals. International journal of obesity 2009, 34 (2), 401-405.

140. Rubin, C.; Capilla, E.; Luu, Y.; Busa, B.; Crawford, H.; Nolan, D.; Mittal, V.; Rosen, C.; Pessin, J.; Judex, S., Adipogenesis is inhibited by brief, daily exposure to high-frequency, extremely low-magnitude mechanical signals. Proceedings of the National Academy of Sciences 2007, 104 (45), 17879-17884.

141. Baskan, O.; Karadas, O.; Mese, G.; Ozcivici, E., Applicability of low-intensity vibrations as a regulatory factor on stem and progenitor cell populations. Current Stem Cell Research & Therapy 2019, 15, 391-399.

142. Prè, D.; Ceccarelli, G.; Visai, L.; Benedetti, L.; Imbriani, M.; Cusella De Angelis, M.; Magenes, G., High-Frequency Vibration Treatment of Human Bone Marrow Stromal Cells Increases Differentiation toward Bone Tissue. Bone marrow research 2013, 2013.

143. Karadas, O.; Mese, G.; Ozcivici, E., Low magnitude high frequency vibrations expedite the osteogenesis of bone marrow stem cells on paper based 3D scaffolds. Biomedical Engineering Letters 2020, 1-11.

144. Baskan, O.; Mese, G.; Ozcivici, E., Low-intensity vibrations normalize adipogenesis-induced morphological and molecular changes of adult mesenchymal stem cells. Proceedings of the Institution of Mechanical Engineers, Part H: Journal of Engineering in Medicine 2017, 231 (2), 160-168.

145. Karadas, O.; Mese, G.; Ozcivici, E., Cytotoxic tolerance of healthy and cancerous bone cells to anti-microbial phenolic compounds depend on culture conditions. Applied biochemistry and biotechnology 2019, 188 (2), 514-526.

146. Fu, Y.; Luo, N.; Klein, R. L.; Garvey, W. T., Adiponectin promotes adipocyte differentiation, insulin sensitivity, and lipid accumulation. Journal of lipid research 2005, 46 (7), 1369-1379.

147. Granlund, L.; Pedersen, J. I.; Nebb, H. I., Impaired lipid accumulation by trans10, cis12 CLA during adipocyte differentiation is dependent on timing and length of treatment. Biochimica et Biophysica Acta (BBA)-Molecular and Cell Biology of Lipids 2005, 1687 (1-3), 11-22.

148. O'Donnell, B. T.; Al-Ghadban, S.; Ives, C. J.; L'Ecuyer, M. P.; Monjure, T. A.; Romero-Lopez, M.; Li, Z.; Goodman, S. B.; Lin, H.; Tuan, R. S., Adipose Tissue-Derived Stem Cells Retain Their Adipocyte Differentiation Potential in Three-Dimensional Hydrogels and Bioreactors. Biomolecules 2020, 10 (7), 1070.

149. Morton, T. L.; Galior, K.; McGrath, C.; Wu, X.; Uzer, G.; Uzer, G. B.; Sen, B.; Xie, Z.; Tyson, D.; Rubin, J.; Styner, M., Exercise Increases and Browns Muscle Lipid in High-Fat Diet-Fed Mice. Frontiers in Endocrinology 2016, 7 (80).

150. Styner, M.; Pagnotti, G. M.; Galior, K.; Wu, X.; Thompson, W. R.; Uzer, G.; Sen, B.; Xie, Z.; Horowitz, M. C.; Styner, M. A.; Rubin, C.; Rubin, J., Exercise Regulation of Marrow Fat in the Setting of PPARγ Agonist Treatment in Female C57BL/6 Mice. Endocrinology 2015, 156 (8), 2753-2761.

151. Qin, Y. X.; Rubin, C. T.; McLeod, K. J., Nonlinear dependence of loading intensity and cycle number in the maintenance of bone mass and morphology. J Orthop Res 1998, 16 (4), 482-9.

152. Rubin, C.; Turner, A. S.; Müller, R.; Mittra, E.; McLeod, K.; Lin, W.; Qin, Y.-X., Quantity and Quality of Trabecular Bone in the Femur Are Enhanced by a Strongly Anabolic, Noninvasive Mechanical Intervention. Journal of Bone and Mineral Research 2002, 17 (2), 349-357.

153. Guniz, B.; Stacie, L.; Hudon, S. F.; Woods, K.; Hayden, E. J.; Xinzhu, P.; Beard, R.; Oxford, J. T.; Gunes, U., Low Intensity Vibrations Augment Mesenchymal

Stem Cell Proliferation and Differentiation Capacity during in vitro Expansion. Scientific Reports (Nature Publisher Group) 2020, 10 (1).

154. Uzer, G.; Pongkitwitoon, S.; Chan, M. E.; Judex, S., Vibration induced osteogenic commitment of mesenchymal stem cells is enhanced by cytoskeletal remodeling but not fluid shear. Journal of biomechanics 2013, 46 (13), 2296-2302.

155. Sun, Q.; Nakata, H.; Yamamoto, M.; Kasugai, S.; Kuroda, S., Comparison of gingiva-derived and bone marrow mesenchymal stem cells for osteogenesis. Journal of cellular and molecular medicine 2019, 23 (11), 7592-7601.

156. Abdallah, B.; Kassem, M., Human mesenchymal stem cells: from basic biology to clinical applications. Gene therapy 2008, 15 (2), 109-116.

157. Chen, P.; Song, M.; Wang, Y.; Deng, S.; Hong, W.; Zhang, X.; Yu, B., Identification of key genes of human bone marrow stromal cells adipogenesis at an early stage. PeerJ 2020, 8, e9484.

158. Devlin, M. J.; Rosen, C. J., The bone–fat interface: basic and clinical implications of marrow adiposity. The Lancet Diabetes & Endocrinology 2015, 3 (2), 141-147.

159. Justesen, J.; Stenderup, K.; Ebbesen, E. N.; Mosekilde, L.; Steiniche, T.; Kassem, M., Adipocyte tissue volume in bone marrow is increased with aging and in patients with osteoporosis. Biogerontology 2001, 2 (3), 165-171.

160. Georgiou, K. R.; Hui, S. K.; Xian, C. J., Regulatory pathways associated with bone loss and bone marrow adiposity caused by aging, chemotherapy, glucocorticoid therapy and radiotherapy. American journal of stem cells 2012, 1 (3), 205.

161. Abdallah, B. M., Marrow adipocytes inhibit the differentiation of mesenchymal stem cells into osteoblasts via suppressing BMP-signaling. Journal of biomedical science 2017, 24 (1), 11.

162. Guerra, D. A.; Paiva, A. E.; Sena, I. F.; Azevedo, P. O.; Batista Jr, M. L.; Mintz, A.; Birbrair, A., Adipocytes role in the bone marrow niche. Cytometry Part A 2018, 93 (2), 167-171.

163. Muruganandan, S.; Roman, A. A.; Sinal, C. J., Adipocyte differentiation of bone marrow-derived mesenchymal stem cells: cross talk with the osteoblastogenic program. Cell Mol Life Sci 2009, 66 (2), 236-53.

164. Rosen, C. J., The epidemiology and pathogenesis of osteoporosis. Endotext [Internet] 2020.

165. Lindsay, R.; Hart, D.; Purdie, D.; Ferguson, M.; Clark, A.; Kraszewski, A., Comparative effects of oestrogen and a progestogen on bone loss in postmenopausal women. Clinical Science and Molecular Medicine 1978, 54 (2), 193-195.

166. Dempster, D. W.; Cosman, F.; Parisien, M.; Shen, V.; Lindsay, R., Anabolic actions of parathyroid hormone on bone. Endocrine reviews 1993, 14 (6), 690-709.

167. Ohlsson, C.; Bengtsson, B.-A. k.; Isaksson, O. G.; Andreassen, T. T.; Slootweg, M. C., Growth hormone and bone. Endocrine reviews 1998, 19 (1), 55-79.

168. Canalis, E.; Delany, A. M., Mechanisms of glucocorticoid action in bone. Annals of the New York Academy of Sciences 2002, 966 (1), 73-81.

169. Beck, B. R.; Kent, K.; Holloway, L.; Marcus, R., Novel, high-frequency, low-strain mechanical loading for premenopausal women with low bone mass: early findings. Journal of bone and mineral metabolism 2006, 24 (6), 505-507.

170. Garman, R.; Rubin, C.; Judex, S., Small Oscillatory Accelerations, Independent of Matrix Deformations, Increase Osteoblast Activity and Enhance Bone Morphology. PLOS ONE 2007, 2 (7), e653.

171. Alizadeh-Meghrazi, M.; Masani, K.; Popovic, M. R.; Craven, B. C., Whole-body vibration during passive standing in individuals with spinal cord injury: effects of plate choice, frequency, amplitude, and subject's posture on vibration propagation. Pm&r 2012, 4 (12), 963-975.

172. Oxlund, B. S.; Ørtoft, G.; Andreassen, T. T.; Oxlund, H., Low-intensity, high-frequency vibration appears to prevent the decrease in strength of the femur and tibia associated with ovariectomy of adult rats. Bone 2003, 32 (1), 69-77.

173. Sun, L.-w.; Luan, H.-q.; Huang, Y.-f.; Wang, Y.; Fan, Y.-b., Effects of local vibration on bone loss in tail-suspended rats. International journal of sports medicine 2014, 35 (07), 615-624.

174. Wehrle, E.; Wehner, T.; Heilmann, A.; Bindl, R.; Claes, L.; Jakob, F.; Amling, M.; Ignatius, A., Distinct frequency dependent effects of whole-body vibration on non-fractured bone and fracture healing in mice. Journal of Orthopaedic Research 2014, 32 (8), 1006-1013.

175. Maloney-Hinds, C.; Petrofsky, J. S.; Zimmerman, G., The effect of 30 Hz vs. 50 Hz passive vibration and duration of vibration on skin blood flow in the arm. Medical Science Monitor 2008, 14 (3), CR112-CR116.

176. Rubinacci, A.; Marenzana, M.; Cavani, F.; Colasante, F.; Villa, I.; Willnecker, J.; Moro, G. L.; Spreafico, L. P.; Ferretti, M.; Guidobono, F.; Marotti, G., Ovariectomy Sensitizes Rat Cortical Bone to Whole-Body Vibration. Calcified Tissue International 2008, 82 (4), 316-326.

177. Slatkovska, L.; Alibhai, S. M.; Beyene, J.; Hu, H.; Demaras, A.; Cheung, A. M., Effect of 12 months of whole-body vibration therapy on bone density and structure in postmenopausal women: a randomized trial. Annals of internal medicine 2011, 155 (10), 668-679.

178. Cardinale, M.; Leiper, J.; Erskine, J.; Milroy, M.; Bell, S., The acute effects of different whole body vibration amplitudes on the endocrine system of young healthy men: a preliminary study. Clinical physiology and functional imaging 2006, 26 (6), 380-384.

179. Uzer, G.; Thompson, W. R.; Sen, B.; Xie, Z.; Yen, S. S.; Miller, S.; Bas, G.; Styner, M.; Rubin, C. T.; Judex, S., Cell Mechanosensitivity to Extremely Low-Magnitude Signals Is Enabled by a LINCed Nucleus. STEM CELLS 2015, 33 (6), 2063-2076.

180. Sykes, J.; Whitescarver, J.; Briggs, L.; Anson, J., Separation of tumor cells from fibroblasts with use of discontinuous density gradients. Journal of the National Cancer Institute 1970, 44 (4), 855-864.

181. Sun, T.; Yan, Z.; Cai, J.; Shao, X.; Wang, D.; Ding, Y.; Feng, Y.; Yang, J.; Luo, E.; Feng, X., Effects of mechanical vibration on cell morphology, proliferation, apoptosis, and cytokine expression/secretion in osteocyte-like MLO-Y4 cells exposed to high glucose. Cell Biology International 2020, 44 (1), 216-228.

182. Waugh, S.; Kashon, M. L.; Li, S.; Miller, G. R.; Johnson, C.; Krajnak, K., Transcriptional pathways altered in response to vibration in a model of hand-arm vibration syndrome. Journal of occupational and environmental medicine/American College of Occupational and Environmental Medicine 2016, 58 (4), 344.

183. Durmus, N. G.; Tekin, H. C.; Guven, S.; Sridhar, K.; Yildiz, A. A.; Calibasi, G.; Ghiran, I.; Davis, R. W.; Steinmetz, L. M.; Demirci, U., Magnetic levitation of single cells. Proceedings of the National Academy of Sciences 2015, 112 (28), E3661-E3668.

184. Grover, W. H.; Bryan, A. K.; Diez-Silva, M.; Suresh, S.; Higgins, J. M.; Manalis, S. R., Measuring single-cell density. Proceedings of the National Academy of Sciences 2011, 108 (27), 10992-10996.

185. Neurohr, G. E.; Amon, A., Relevance and Regulation of Cell Density. Trends in Cell Biology 2020, 30 (3), 213-225.

186. Nerurkar, N. L.; Elliott, D. M.; Mauck, R. L., Mechanics of oriented electrospun nanofibrous scaffolds for annulus fibrosus tissue engineering. Journal of Orthopaedic Research 2007, 25 (8), 1018-1028.

187. Wang, X.; Yu, D.-G.; Li, X.-Y.; Bligh, S. A.; Williams, G. R., Electrospun medicated shellac nanofibers for colon-targeted drug delivery. International journal of pharmaceutics 2015, 490 (1-2), 384-390.

188. Potrč, T.; Baumgartner, S.; Roškar, R.; Planinšek, O.; Lavrič, Z.; Kristl, J.; Kocbek, P., Electrospun polycaprolactone nanofibers as a potential oromucosal delivery system for poorly water-soluble drugs. European Journal of Pharmaceutical Sciences 2015, 75, 101-113.

189. Oliveira, M. F.; Suarez, D.; Rocha, J. C. B.; de Carvalho Teixeira, A. V. N.; Cortés, M. E.; De Sousa, F. B.; Sinisterra, R. D., Electrospun nanofibers of polyCD/PMAA polymers and their potential application as drug delivery system. Materials Science and Engineering: C 2015, 54, 252-261.

190. Aytac, Z.; Sen, H. S.; Durgun, E.; Uyar, T., Sulfisoxazole/cyclodextrin inclusion complex incorporated in electrospun hydroxypropyl cellulose nanofibers as drug delivery system. Colloids and Surfaces B: Biointerfaces 2015, 128, 331-338.

191. Ghasemi-Mobarakeh, L.; Prabhakaran, M. P.; Morshed, M.; Nasr-Esfahani, M.-H.; Ramakrishna, S., Electrospun poly (ε-caprolactone)/gelatin nanofibrous scaffolds for nerve tissue engineering. Biomaterials 2008, 29 (34), 4532-4539.

192. Xu, C.; Inai, R.; Kotaki, M.; Ramakrishna, S., Aligned biodegradable nanofibrous structure: a potential scaffold for blood vessel engineering. Biomaterials 2004, 25 (5), 877-886.

193. Guo, Z.; Xu, J.; Ding, S.; Li, H.; Zhou, C.; Li, L., In vitro evaluation of random and aligned polycaprolactone/gelatin fibers via electrospinning for bone tissue engineering. Journal of Biomaterials Science, Polymer Edition 2015, 26 (15), 989-1001.

194. McCullen, S. D.; Autefage, H.; Callanan, A.; Gentleman, E.; Stevens, M. M., Anisotropic fibrous scaffolds for articular cartilage regeneration. Tissue Engineering Part A 2012, 18 (19-20), 2073-2083.

195. Meng, Z.; Wang, Y.; Ma, C.; Zheng, W.; Li, L.; Zheng, Y., Electrospinning of PLGA/gelatin randomly-oriented and aligned nanofibers as potential scaffold in tissue engineering. Materials Science and Engineering: C 2010, 30 (8), 1204-1210.

196. Banes, A. J.; Tsuzaki, M.; Yamamoto, J.; Brigman, B.; Fischer, T.; Brown, T.; Miller, L., Mechanoreception at the cellular level: the detection, interpretation, and diversity of responses to mechanical signals. Biochemistry and Cell Biology 1995, 73 (7-8), 349-365.

197. Anil-Inevi, M.; Yaman, S.; Yildiz, A. A.; Mese, G.; Yalcin-Ozuysal, O.; Tekin, H. C.; Ozcivici, E., Biofabrication of in situ self assembled 3D cell cultures in a weightlessness environment generated using magnetic levitation. Scientific reports 2018, 8 (1), 7239.

198. Sangsanoh, P.; Suwantong, O.; Neamnark, A.; Cheepsunthorn, P.; Pavasant, P.; Supaphol, P., In vitro biocompatibility of electrospun and solvent-cast chitosan substrata towards Schwann, osteoblast, keratinocyte and fibroblast cells. European Polymer Journal 2010, 46 (3), 428-440.

199. Jaiswal, A.; Chhabra, H.; Soni, V.; Bellare, J., Enhanced mechanical strength and biocompatibility of electrospun polycaprolactone-gelatin scaffold with surface deposited nano-hydroxyapatite. Materials Science and Engineering: C 2013, 33 (4), 2376-2385.

200. Qi, H.; Ye, Z.; Ren, H.; Chen, N.; Zeng, Q.; Wu, X.; Lu, T., Bioactivity assessment of PLLA/PCL/HAP electrospun nanofibrous scaffolds for bone tissue engineering. Life sciences 2016, 148, 139-144.

201. Abdal-hay, A.; Hamdy, A. S.; Khalil, K. A., Fabrication of durable high performance hybrid nanofiber scaffolds for bone tissue regeneration using a novel, simple in situ deposition approach of polyvinyl alcohol on electrospun nylon 6 nanofibers. Materials Letters 2015, 147, 25-28.

202. Lin, W.-H.; Yu, J.; Chen, G.; Tsai, W.-B., Fabrication of multi-biofunctional gelatin-based electrospun fibrous scaffolds for enhancement of osteogenesis of mesenchymal stem cells. Colloids and Surfaces B: Biointerfaces 2016, 138, 26-31.

203. Nagarajan, S.; Belaid, H.; Pochat-Bohatier, C.; Teyssier, C.; Iatsunskyi, I.; Coy, E.; Balme, S.; Cornu, D.; Miele, P.; Kalkura, N. S., Design of Boron Nitride/Gelatin

Electrospun Nanofibers for Bone Tissue Engineering. ACS applied materials & interfaces 2017, 9 (39), 33695-33706.

204. Frank W Booth 1 , C. K. R., Matthew J Laye, Lack of Exercise Is a Major Cause of Chronic Diseases. In Comprehensive Physiology, 2012; pp 1143-1211.

205. Mao, A. S.; Shin, J.-W.; Mooney, D. J., Effects of substrate stiffness and cell-cell contact on mesenchymal stem cell differentiation. Biomaterials 2016, 98, 184-191.

VITA

Date and place of birth: 22/03/1989 İzmir

Education:

MSc: Izmir Institute of Technology, Biotechnology

BSc: Izmir Institute of Technology, Molecular Biology and Genetics

Fellowships & Honors:

Erasmus Scholarship, Università di Modena e Reggio Emilia, June-September 2010

Publications:

Thesis:

Molecular Characterization of Adult Stem Cells' Adaptations to Mechanical Signals During Adipogenic Commitment. Msc.Thesis, Department of Biotechnology, IZTECH, 2015

Articles in International Journals:

Ince Yardimci, A., Baskan, O., Yilmaz, S., Mese, G., Ozcivici, E., & Selamet, Y. "Osteogenic differentiation of mesenchymal stem cells on random and aligned PAN/PPy nanofibrous scaffolds". Journal of biomaterials applications, 34(5), 640-650, 2019

Baskan O., Karadas O., Mese G., Ozcivici E., "Applicability of Low-Intensity Vibrations as a Regulatory Factor on Stem and Progenitor Cell Populations" Current Stem Cell Research & Therapy, 15(5), 391-399, 2020

Baskan O., Mese G., Ozcivici E. "Low-intensity vibrations normalize adipogenesis-induced morphological and molecular changes of adult mesenchymal stem cells." Journal of Engineering in Medicine, 231(2):160-168, 2017

M. Olcum, O. Baskan, O. Karadas, E. Ozcivici. Application of Mechanical Vibrations for Bone Tissue Maintenance and Regeneration. Turkish Journal of Biology, Volume 40, pages 300-307, February 2016